



**KAUNO TECHNOLOGIJOS UNIVERSITETAS
CHEMINĖS TECHNOLOGIJOS FAKULTETAS**

Matas Steponaitis

**ORGANINIAI PIRIDINIO IR KETVIRTINIO AMONIO
DARINIAI: SINTEZĖ IR PUSLAIDININKINIŲ SAVYBIŲ
TYRIMAS**

Baigiamasis magistro darbas

Vadovas

doc. dr. Tadas Malinauskas

Kaunas, 2017



**KAUNAS UNIVERSITY OF TECHNOLOGY
FACULTY OF CHEMICAL TECHNOLOGY**

Matas Steponaitis

**DERIVATIVES CONTAINING PYRIDINIUM AND
QUATERNARY AMMONIUM MOIETIES: SYNTHESIS
AND INVESTIGATION OF THE SEMICONDUCTING
PROPERTIES**

Master's thesis

Supervisor

Assoc. Prof. Dr. Tadas Malinauskas

Kaunas, 2017

KAUNO TECHNOLOGIJOS UNIVERSITETAS
CHEMINĖS TECHNOLOGIJOS FAKULTETAS
ORGANINĖS CHEMIJOS KATEDRA

ORGANINIAI PIRIDINIO IR KETVIRTINIO AMONIO
DARINIAI: SINTEZĖ IR PUSLAIDININKINIŲ SAVYBIŲ
TYRIMAS

Baigiamasis magistro darbas

Studijų programa Taikomoji chemija (kodas 612F10003)

Vadovas

Doc. Dr. Tadas Malinauskas

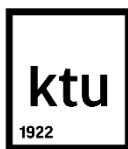
Recenzentas

Dr. Dalius Gudeika

Darbą atliko

Matas Steponaitis

Kaunas, 2017



KAUNO TECHNOLOGIJOS UNIVERSITETAS
CHEMINĖS TECHNOLOGIJOS FAKULTETAS

Matas Steponaitis

Studijų programa Taikomoji chemija (kodas 621F10003)

Baigiamojo darbo „Organiniai piridinio ir ketvirtinio amonio dariniai: sintezė ir puslaidininkinių savybių tyrimas“

AKADEMINIO SAŽININGUMO DEKLARACIJA

2017 m. _____ mėn. __ d.

Kaunas

Patvirtinu, kad mano **Mato Steponaičio** baigiamasis darbas tema „Organiniai piridinio ir ketvirtinio amonio dariniai: sintezė ir puslaidininkinių savybių tyrimas“ yra parašytas visiškai savarankiškai, o visi pateikti duomenys ar tyrimų rezultatai yra teisingi ir sąžiningai gauti. Šiame darbe nei viena darbo dalis nėra plagijuota nuo jokių spausdintinių ar internetinių šaltinių, visos kitų šaltinių tiesioginės ir netiesioginės citatos nurodytos literatūros nuorodose. Įstatymu nenumatytų piniginių sumų už šį darbą niekam nesu mokėjęs.

Aš suprantu, kad išaiškėjus nesąžiningumo faktui, man bus taikomos nuobaudos, remiantis Kauno technologijos universitete galiojančia tvarka.

(studento vardas ir pavardė, įrašyti ranka)

(parašas)

Contents

Santrauka.....	6
Summary	7
List of abbreviations.....	8
1. Introduction	1
2. Literature review	2
2.1 Perovskite solar cells	2
2.2 Basic requirements for hole transporting materials.....	3
2.3 Spiro-MeOTAD.....	4
2.4 Additive-free low molecular weight compounds	6
2.5 Polymeric hole transporting materials.....	9
2.6 Organic mixed-valence and quaternary ammonium compounds	12
2.7 Literature review conclusions.....	15
3. Results and discussion.....	16
3.1 Synthesis of model compounds	16
3.2 Synthesis of pyridine containing Spiro-MeOTAD and V886 derivatives.....	18
3.3 Synthesis of triphenylamine based ionic hole transporting materials	20
3.4 Thermal properties of synthesized materials	22
3.5 Optical properties of synthesized materials.....	25
3.6 Photoelectric properties of investigated materials.....	27
4. Experimental details	31
4.1 General Methods and Materials.....	31
4.2 Description of synthesis.....	32
5. Results and conclusions	44
List of publications.....	45
Acknowledgments.....	46
References	47

Steponaitis, M. ORGANINIAI PIRIDINIO IR KETVIRTINIO AMONIO DARINAI: SINTEZĖ IR PUSLAIDININKINIŲ SAVYBIŲ TYRIMAS. *Magistro* baigiamasis darbas / vadovas doc. dr. Tadas Malinauskas; Kauno technologijos universitetas, Cheminės technologijos fakultetas, Organinės chemijos katedra.

Mokslo kryptis ir sritis: fiziniai mokslai, chemija.

Reikšminiai žodžiai: organiniai puslaidininkiai, perovskitas, saulės celės.

Kaunas, 2017. 58 p.

Santrauka

Senkant iškastinio kuro atsargoms, didėjant pasauliniam energijos poreikiui ir užterštumui dėl pasenusių energijos generavimo technologijų, reikalinga nauja alternatyva, kuri patenkintų žmonijos poreikius nesukeldama negatyvių padarinių aplinkai. Todėl neturėtų būti keista, jog mokslininkų dėmesys krypsta į įvairias atsinaujinančios energijos rūšis. Viena iš jų yra saulės energija, kadangi per 1 minutę saulė išspinduliuoja daugiau nei 10^{15} W energijos, tiek pakaktų visai žmoneijai vieneriems metams. Tokie įspūdingi duomenys skatina mokslininkus kurti vis tobulesnius prietaisus, kurie saulės skleidžiamą energiją galėtų paversti elektros energija. Vieni iš tokių prietaisų yra saulės elementai, tačiau kol kas daugumos jų gamybos technologijos yra sudėtingos ir reikalaujančios daug resursų. Dabartinė chemijos užduotis – sukurti naujos kartos medžiagas, tinkančias našių saulės celių konstravimui. Minėti įrenginiai dažnai sudaromi iš kelių, įvairias funkcijas atliekančių, medžiagų sluoksnių, kurių kiekvienam keliami tam tikri reikalavimai. Šio darbo tikslas buvo susintetinti organinės kilmės *p*-tipo puslaidininkinius junginius (HTM) ir pritaikyti juos perovskitinių saulės elementų konstravimui. Tokie junginiai privalo pasižymėti geru laidumu, tinkamu jonizacijos potencialu, bei neaukšta gamybos savikaina.

Šio darbo metu buvo susintetinti nauji, iki šiol literatūroje neaprašyti, ketvirtines amonio grupes turintys organiniai junginiai, iširtos jų terminės, optinės ir fotoelektrinės savybės bei šių savybių pokytis prijungiant arba pakeičiant jonines grupes. Buvo pastebėta, kad ketvirtinio amonio grupių įvedimas keičia medžiagų optines savybes, tačiau lyginant tos pačios grupės joninius junginius tarpusavyje pokytis matomas nežymus. Verta paminėti, jog įvedus jonines grupes pakyla junginio jonizacijos potencialas (I_p), taipogi kinta ir terminės joninių puslaidininkinių savybės. Manoma, kad tokių darinių parametrai priklauso nuo prijungtų jonų prigimties ir molekulinė orbitalių delokalizacijos aplink ketvirtinio amonio grupes.

Išanalizavus gautus duomenis buvo padarytos išvados, kad dėl žemos stiklėjimo temperatūros (T_g), bei prasto laidumo ir suderinamumo su kitais saulės elemento sluoksniais, susintetinti junginiai negali būti panaudoti našių saulės celių konstravimui, tai patvirtina ir gauti prietaisų rezultatai. Nepaisant to gauta vertinga informacija apie šių junginių sintezę, bei terminių ir optoelektrinių savybių pokyčius kintant molekulinei struktūrai bus vertinga kuriant naujus organinius puslaidininkius.

Steponaitis, M. *DERIVATIVES CONTAINING PYRIDINIUM AND QUATERNARY AMMONIUM MOIETIES: SYNTHESIS AND INVESTIGATION OF SEMICONDUCTING PROPERTIES*: Master's thesis in Chemistry / supervisor assoc. prof. Tadas Malinauskas. The Faculty of Chemical Technology, Kaunas University of Technology.

Research area and field: Physical Sciences, chemistry

Key words: organic semiconductors, perovskite, solar cell.

Kaunas, 2017. 58 p.

Summary

The gradual depletion of Earth's natural resources, the world's growing energy needs and worldwide pollution, demands a new way of generating clean energy for mankind. Therefore, it should not come as a surprise, that renewable resources are now the most attractive option to replace fossil fuel. One of the most promising source of energy is the sun. It emits enough energy (in one minute around 10^{15} W) to supply the entire world's demand and attracts the attention of scientists around the world. To make use of such vast amount of energy solar cell devices are being used, but the technology behind it is rather complicated and costly. To help perfect and cheapen the technology behind it chemistry has to offer new generation materials designed to fit all the criteria for efficient solar cell fabrication. Aforementioned devices are usually made out of layers, that are all responsible for different functions. The goal of this work was to synthesize organic p-type semiconductors and use them in perovskite solar cells. Compounds created for this purpose have to have good conductivity, correct ionization potential and a low production cost.

In this work, synthesis of new organic ionic materials and the investigation of their thermal, optical, and photoelectric properties is described. It was observed that the addition of ionic groups changes optical properties of a compound, however this change is small between semiconductors of the same group, that differs only by the attached anion. Furthermore, adding ions leads to an increase in ionization potential and changes the thermal properties of the material. It is suspected that such a change occurs because of the nature of the ions and the delocalization of molecular orbitals around ionic groups.

After analyzing the collected data, it can be concluded that low glass transition temperature (T_g), poor conductivity and overall low device efficiencies the obtained ionic compounds cannot be used in solar cell fabrication. Despite that, the acquired information about the synthesis and changes in ionic material properties due to variation of their structure, is valuable for further research in organic HTMs for perovskite solar cells.

List of abbreviations

<i>PSC</i>	<i>Perovskite solar cell;</i>
<i>HTM</i>	<i>Hole transporting material;</i>
<i>DSSC</i>	<i>Dye sensitized solar cells;</i>
<i>SEM</i>	<i>Scanning electron microscopy;</i>
<i>TiO₂</i>	<i>Titanium dioxide;</i>
<i>FTO</i>	<i>Fluorinated tin oxide</i>
<i>eV</i>	<i>Electron-volt</i>
<i>I_p</i>	<i>Ionization potential</i>
<i>HOMO</i>	<i>Highest occupied molecular orbital</i>
<i>μ</i>	<i>charge carrier mobility</i>
<i>T_g</i>	<i>Glass transitioning temperature</i>
<i>LiTFSI</i>	<i>Lithium bistrifluoromethanesulfonimide</i>
<i>TBP</i>	<i>4-tert-butylpyridine</i>
<i>VIS</i>	<i>Visible</i>
<i>PCE</i>	<i>Power conversion efficiency</i>
<i>HCP</i>	<i>Hole conducting polymer</i>
<i>PF</i>	<i>Polyfluorene</i>
<i>M.W.</i>	<i>Molecular weight</i>
<i>ETM</i>	<i>Electron transporting material.</i>
<i>TPA</i>	<i>Triphenylamine</i>
<i>MeOTPA</i>	<i>Methoxy triphenylamine</i>
<i>MV</i>	<i>Mixed-valence</i>
<i>D-A</i>	<i>Donor-acceptor</i>
<i>ET</i>	<i>Electron transfer</i>
<i>CT</i>	<i>Charge transfer</i>
<i>MAI</i>	<i>Methylammonium iodide</i>
<i>T_m</i>	<i>Melting point</i>
<i>LUMO</i>	<i>Lowest unoccupied molecular orbital</i>
<i>DCM</i>	<i>Dichloromethane</i>
<i>DMF</i>	<i>Dimethylformamide</i>
<i>DMSO</i>	<i>Dimethyl sulfoxide</i>
<i>THF</i>	<i>Tetrahydrofuran</i>
<i>TPA</i>	<i>Triphenylamine</i>
<i>TLC</i>	<i>Thin layer chromatography</i>
<i>MW</i>	<i>Microwave</i>
<i>σ</i>	<i>Conductivity</i>
<i>V_{oc}</i>	<i>Open circuit voltage</i>
<i>J_{sc}</i>	<i>Short circuit current</i>
<i>FF</i>	<i>Fill factor</i>

1. Introduction

From the late 18 century till now humanity made an enormous leap forwards, due to the rapid development of technologies such as: the invention of a cars, computers, space shuttles, automatic production lines etc. All these inventions need energy to work and as the human population keeps expanding, the demand for energy will be rising as well. Furthermore, we cannot rely on our old energy sources (coal, nuclear energy) as the by-products of these process are polluting our planet. So, a clean energy alternative is a great source for powering our everyday world.

From all the alternative energy options, the most promise is shown by the photovoltaics systems, which convert solar energy into electrical energy via solar panels. Currently one of the most widely produced photovoltaic devices are crystalline silicon cells, but their production processes are difficult and the cost is quite higher compared to the price of fossil fuel [1]. Organic chemistry gives us tools required for creation of new generation of solar cells. One of the most promising photovoltaic device is the solid-state hybrid perovskite solar cell (PSC), efficiency of which has improved, from 3.8% to 21.8% in eight years span [2].

The main aim of the thesis:

Synthesize organic hole transporting molecules with ionic moieties in their structure.

Tasks proposed to achieve the aim:

- synthesis of model materials with heterocycle pyridine rings in their structure.
- synthesis of ionic compounds.
- investigation of thermal, photoelectric and electrochemical properties of the synthesized materials and exploring the influence of molecular structure on said properties
- testing the synthesized materials in solid-state hybrid solar cells.

2. Literature review

As briefly mentioned in the introduction, perovskite solar cells enjoyed rapid success in a short period of time. That alone makes it an interesting topic for researchers around the world. However, the path to commercially produced product is not that easy and requires solution of some fundamental technological difficulties, like perovskite stability issues or upscaling problems. Both limitations can be solved by synthesizing cheap, efficient and stable HTM. Before trying to achieve this goal, it would be wise to check and analyze the most important existing research on materials used for photovoltaic devices, mainly perovskite solar cells.

2.1 Perovskite solar cells

The name Perovskite was given to a mineral of calcium titanium oxide (CaTiO_3) discovered in 1839 by Gustav Rose in Ural mountains of Russia and named after Russian mineralogist Lev Perovski. When we talk about perovskites we are referring to a class of materials with the general formula ABX_3 . In PSC applications the structure ABX_3 usually can be broken down to an anion X (like Cl, Br or I), and cations A and B which are of different sizes (A being bigger than B, for example A could be methyl ammonium ion- $(\text{CH}_3\text{NH}_3)^+$ and B – lead or tin) [3;4]. Under ideal conditions perovskites form a specific cubical structure shown in **Figure 1**.

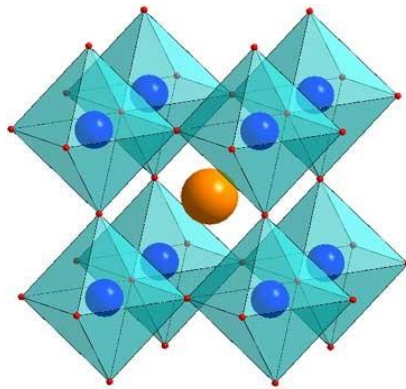


Figure 1 Crystal lattice structure of cubical perovskite ABX_3 .

Orange sphere symbolizes A, blue sphere B and the red dots X

A strong impact on the construction of the photovoltaic devices was made, when researchers realised that a perovskite layer can substitute the organic dye layer in DSSC. The versatile preparation of different perovskite structures [5] makes it a unique material for photoelectronic applications. Layers made from it possess bipolar charge mobility, long exciton lifetime and high absorption coefficient which allowed PSC to achieve an efficiency of 22.1% in a short period of time [6]. This rapid development is quite impressive considering that silicon solar cells reached 25.6% efficiency in many decades.

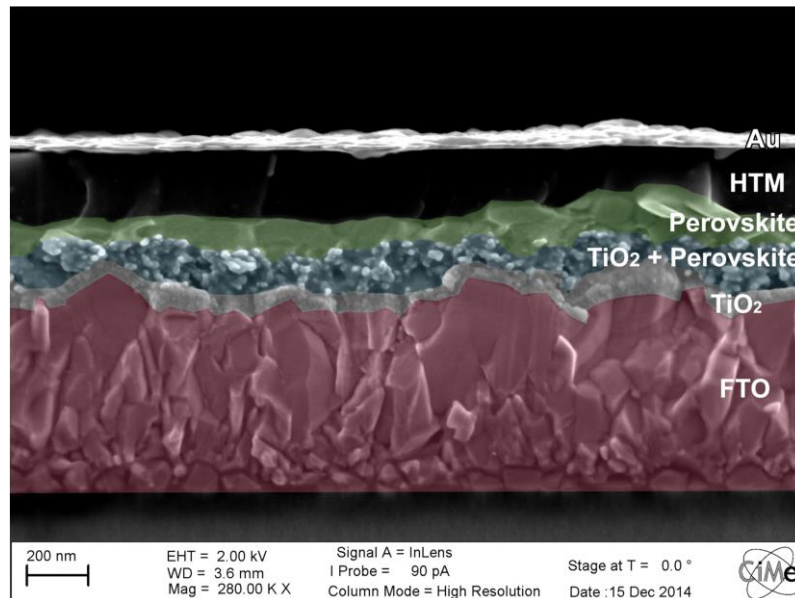


Figure 2. Cross section of perovskite solar cell under SEM

The PSC itself is usually made out of six layers, all with different purpose (**Figure 2**). It is of great importance to address the functions of every layer from top to bottom. On the top is a gold cathode (can be silver as well) and its function is to collect positive charges, below it there's a hole transporting material. The next two layers are perovskite layer (light absorbing material) and perovskite mixed with TiO₂ (improves the migration of electrons towards anode) respectively. The last two parts of PSC are TiO₂, the electron transporting material, and FTO – the anode, which collects electrons.

2.2 Basic requirements for hole transporting materials

For charge transport to occur in HTM, it must have at least one electron donating group and a relatively low I_p , which can be tuned by the addition of donor groups [7].

Ionization potential itself is a parameter that defines the minimum amount of work necessary to remove an electron from a molecule's highest occupied molecular orbital (HOMO) [8]. I_p also must fit in a certain interval, if a high efficiency is the goal (for hole transporting materials used in PSC devices it is around 4.9-5.4eV). Besides I_p , a proper HTM has to have a good ability to form thin films, high charge carrier mobility, electrochemical, morphological and thermal stability, also good conductivity is a desirable characteristic as well. Achieving all these goals is not an easy task, considering that most of the above-mentioned parameters must be balanced among themselves.

Good quality thin films are essential for a high performance solid state solar cell. The structure of the film cannot contain any impurities or defects, it must be uniform in order to reach high device efficiency. This is obtainable by using highly soluble amorphous compounds,

which have the advantage against crystalline materials due to the spontaneous and uncontrollable crystallization of the later (this causes charge trapping which results in a drop of efficiency).

A key figure in determining an organic molecules tendency to form amorphous structure is the glass transitioning temperature. It was observed that materials with higher T_g values and certain molecular structures are more likely to form amorphous layers when rapidly cooled as well as maintaining them for longer. A set of rules for quality layer formation are described below:

- i. Symmetrical molecules more often than none form crystals
- ii. Introduction of long aliphatic chains helps to improve morphological stability and the integrity of a layer
- iii. Higher T_g is achieved if the structure is large and rigid [9].

High charge carrier mobility (μ) is another very important parameter for an efficient semiconductor. It is described as the distance that a single charge travels while being pulled by an electrical field which magnitude (E) equals 1, per unit of time. The charge carrier mobility differs by the change in external electrical field (E), pressure (P), temperature (T) or the spatial structure of the molecule (the more orderly the structure is the faster the charge travels) [10]. For example, the highest charge drift mobility can be found in single crystals, while in amorphous materials charges usually travel slower.

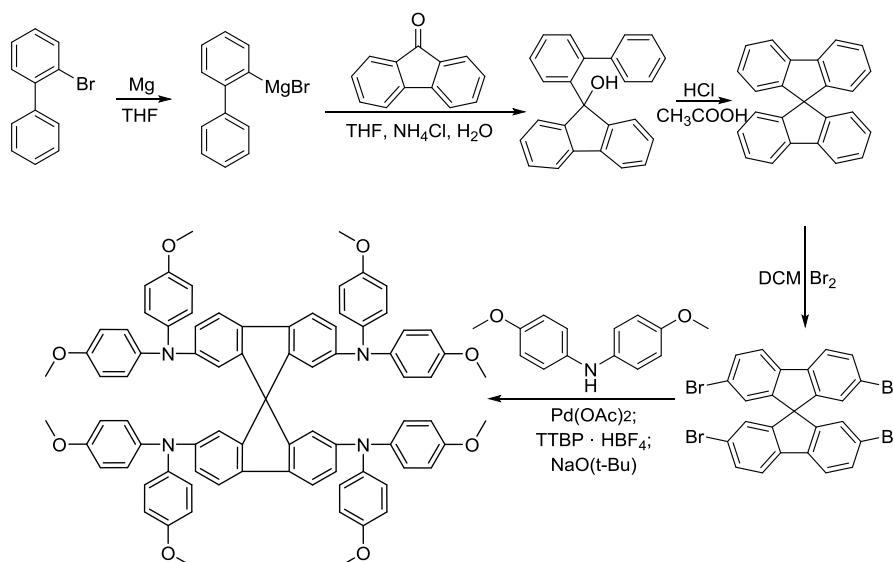
As it was said earlier, good conductivity (σ) is required as well. It measures the amount of charged particles that move in the applied electric field - more moving charges means higher σ . Conductivity itself is highly intertwined with charge carrier mobility, in best case scenario an HTM should have a reasonable amount of charged particles that have high μ , but that doesn't mean that a molecule with high σ will have fast moving holes.

In real life applications a perfect hole transporting material does not really exist. Usually it is a compromise between parameters. That's why designing new efficient materials is a challenging task.

2.3 Spiro-MeOTAD

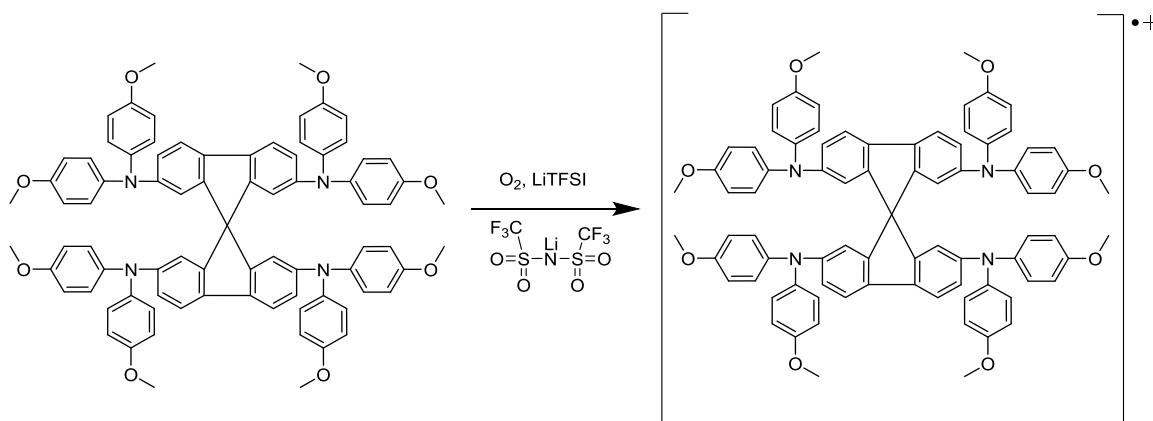
In 2012, an organic HTM spiro-MeOTAD (2,2',7,7'-tetrakis-[*N,N*-di(4-methoxyphenyl)amino]-9,9'-spirobifluorene), was applied in perovskite solar cell for the very first time [11] and it is still the most widely used HTM till this day. Spiro-MeOTAD got its popularity for his low ionization potential, good solubility and stability. Aforementioned properties of this compound allowed the rapid development of PSC. Despite such good performance spiro-MeOTAD has its drawbacks.

For starters, the synthesis is not easy or cheap. It consists of 5 steps using expensive materials and harsh reaction conditions (**Scheme 1**).



Scheme 1. Synthesis of spiro-MeOTAD

Spiro-MeOTAD works in a solar cell only when it is doped. During doping the conductivity changes due to the partial oxidation of the compound. In spiro-MeOTAD case carbocation is formed [12] (the same rule applies to the majority of the organic HTMs used in photovoltaics). The doping procedure is usually carried out using lithium bistrifluoromethanesulfonimide (LiTFSI) in an oxygen containing environment (**Scheme 2**).



Scheme 2 Doping of Spiro-MeOTAD

The alteration of spiro-MeOTAD conductivity and UV/VIS absorption spectra are shown in **Figure 3**. A key figure in this experiment is oxygen, without it carbon radicals could not form, therefore there would not be any change in the electric properties of the HTM [13]. From the demonstrated data, we can come to a conclusion that there is an optimal amount of LiTFSI salt (roughly 18%) needed to reach the highest conductivity, anything above it will lower down the compounds ability to conduct electrical current. However, the concentration of the lithium salt affects the absorption spectra differently: the higher the concentration the higher the absorption maximum.

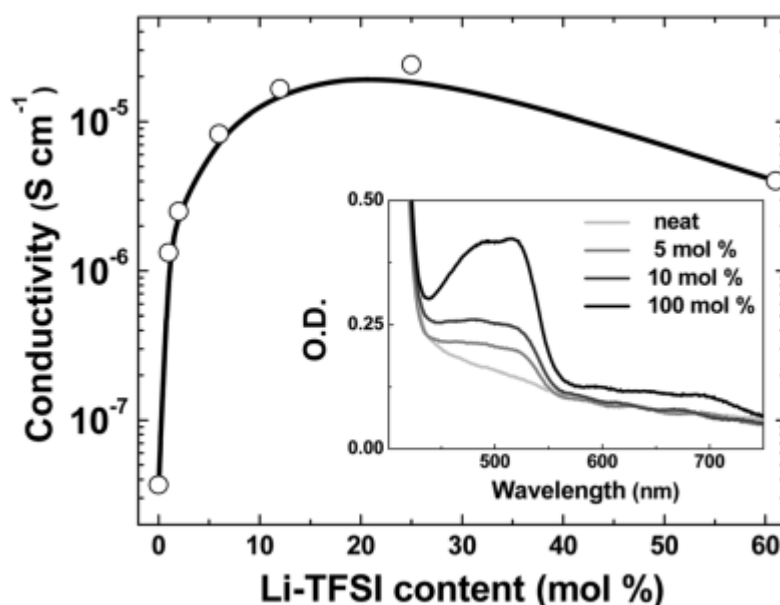


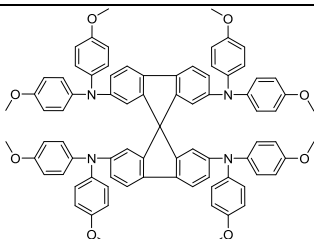
Figure 3. Spiro-MeOTAD absorption and conductivity dependence on Li-TFSI concentration

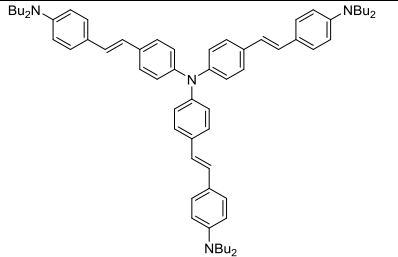
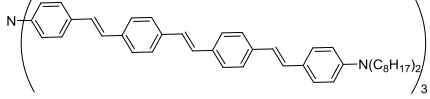
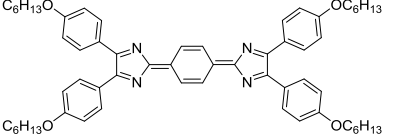
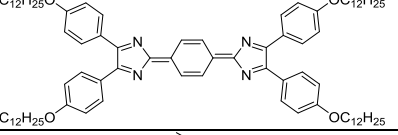
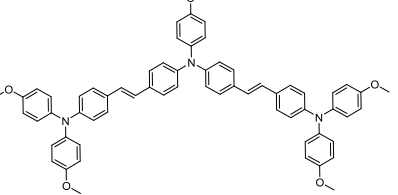
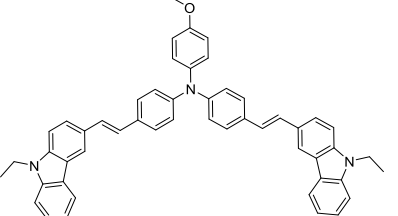
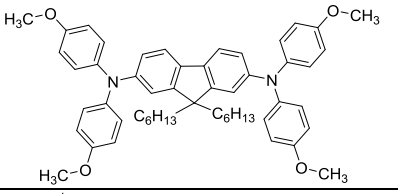
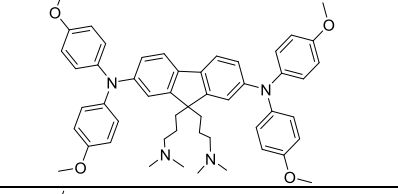
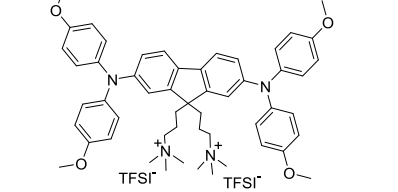
The doping process itself is flawed: it is hard to control the compounds oxidation, small lithium ions can migrate to other layers of the device, lowering the performance, also Li-TFSI is very hygroscopic, which means it will allow moisture to penetrate to the perovskite layer leading to the degradation of the later [13]. Solution to these problems could be utilization of cheaper and dopant-free HTM.

2.4 Additive-free low molecular weight compounds

The HTM oxidation process and the constant stability issues caused by it prompted the search of additive free HTMs. However, in many cases when creating efficient charge transporting materials there are some obstacles to be considered: either the synthesis path is long and difficult or the cost of the product is too high. Therefore, in this chapter we review the compounds not only by their efficiency but also by the possibility of commercial applications as well.

Table 1. Low molecular weight HTMs

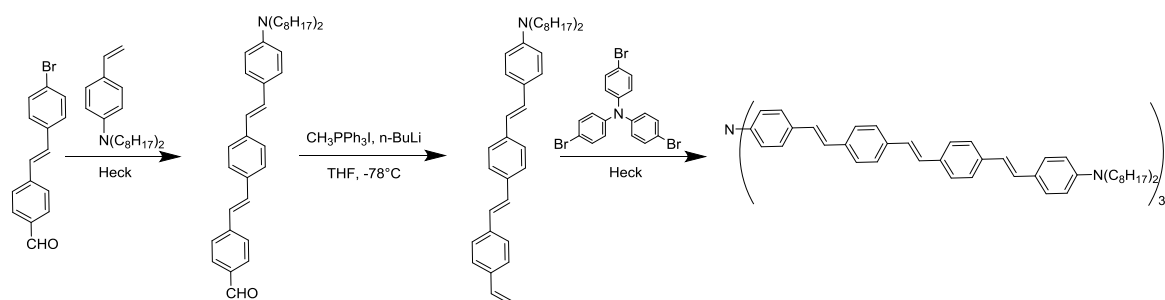
Compounds name or abbreviation	HTM	V_{oc} , V	J_{sc} , mA/c m ²	FF, %	PCE, %.	Reference
Spiro-MeOTAD		1.08	21.26	75	16.6-21	[14]

ST1		1.05	21.04	65	15.0	[15]
TP1		0.96	20.23	63	12.6	[16]
DIQ-C6		0.91	15.86	54	7.8	[17]
DIQ-C12		0.95	19.84	65	12.2	[17]
Z34		1.05	21.27	69	15.9	[18]
Z35		0.98	18.02	58	10.8	[18]
AS37		1.06	20.05	37	7.8	[19]
X41		0.92	0.58	15	0.1	[19]
X44		1.08	15.2	67	15.2	[19]

One of the most widely used structure for designing new HTMs is tr_p henylamine (TPA). Its fragments can be seen in compounds coded as ST1, TP1 and Z34 (**Table 1**). The foremost can

be acquired by one step Heck reaction of the inexpensive commercial precursors with a high yield. Devices made with 4-(4-(bis(4-(4-(dibutylamino)styryl)phenyl)-amino)styryl)-N,N-dibutylaniline (ST1) have exhibited average efficiency of 15% [15].

In a work published by P. Qi *et al.* [16], HTM similar to the structure of ST1 have been synthesized. Using a three-step synthesis, expensive reagents and harsh conditions they have managed to synthesise a TPA derivative TP1 (**Scheme 3**). In comparison to the structure of ST1, the previously mentioned TP1 has a longer conjugated system and longer aliphatic chains at the ends, but despite all that TP1 exhibits lower efficiency (12.6%) and is arguably an unsuitable candidate for a PSC application.



Scheme 3. Synthesis of TP1

Another additive-free HTM is Z34, which belongs to a group of methoxy triphenylamine derivatives (MeOTPA). This compound was acquired using a Wittig reaction with cheap starting materials. As a result, Z34 is a lot cheaper than widely used spiro-MeOTAD and devices with Z34 show efficiency of almost 16%. In the same article published by F. Zhang *et al.*, they have reported synthesis of compound Z35, that differ from Z34 by the addition of two carbazole derivatives instead of two TPA moieties. The efficiencies of the tested perovskite devices containing Z35 were lower by 5% than that of Z34 [18].

Synthesis of quinoid-based hole transporting materials with a rigid quinoid core [3,6-di(2H-imidazol-2-ylidene)-cyclohexa-1,4-diene] (DIQ-C6 and DIQ-C12) was inspired by similar compounds exhibiting good thermal stability, planar core favoring intermolecular electronic coupling and intense light absorption in the long wavelength region. The acquired compounds are among the rare examples of HTMs absorbing intensely in the red–near-infrared region [17]. Though perovskite with a structure of MAPbI₃ has broad absorption in the visible region, the absorption becomes weaker after 600 nm. Therefore, the strong absorption of DIQ compounds can complement the absorption of MAPbI₃ in this region. DIQ-C6 and DIQ-C12 differ from one another just by the length of aliphatic chains (**Table 1**), but the difference in efficiency is more than 4% in the favor of DIQ-C12.

A group of fluorene based compounds AS37, X41, X44 demonstrates how the power conversion efficiency (PCE) is affected by the change of an aliphatic chain and addition of ionic

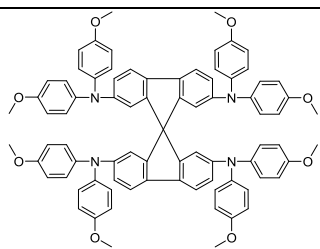
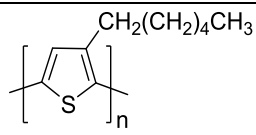
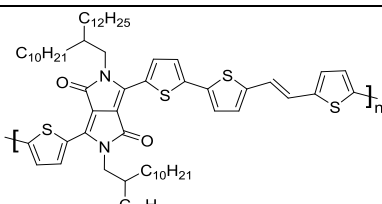
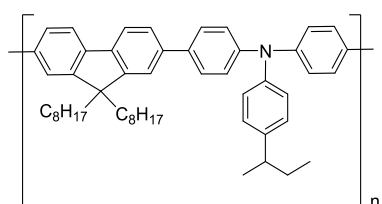
moieties. The foremost compound has hexyl aliphatic chains and exhibits device efficiency of 7.8%, however the change of alkyl to *N,N*-dimethylpropylamine lowers the PCE to 0.1%. The addition of a methyl group and TFSI counter ions to X41 helped to create an ionic compound X44. This change significantly enhanced the hole conductivity that lead to the increase of efficiency to 15.2% [19].

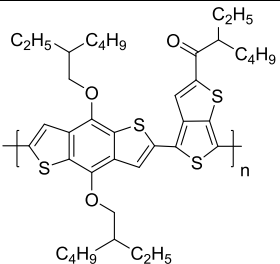
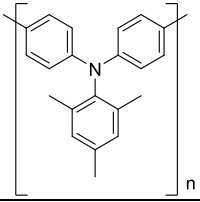
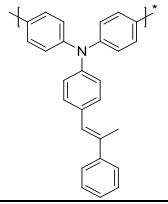
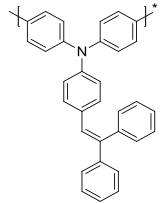
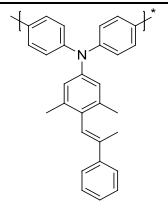
All the above mentioned HTMs enhanced the stability of their respective PSCs due to the absence of hygroscopic LiTFSI and other dopants. Furthermore, ST1 and Z34 showed a drop in all photovoltaic parameters when additives were introduced. Taking into consideration their low production cost it makes ST1 and Z34 an attractive alternative for spiro-MeOTAD.

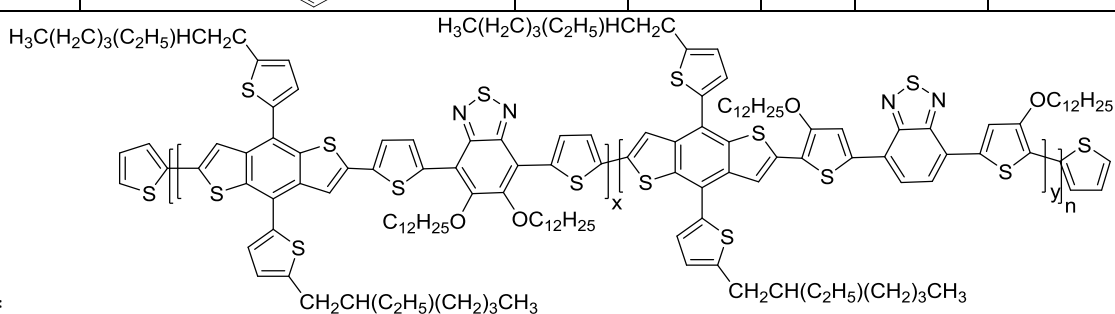
2.5 Polymeric hole transporting materials

At the dawn of PSC, the most widely used polymeric hole transporting material for organic or hybrid photovoltaic cells was P3HT (Poly(3-hexylthiophene-2,5-diyl)). But its low hole mobility and high production cost, made scientists look for better alternatives. In some cases, this search produced a variety of different new compounds and in other cases it only meant re-using known compounds in the devices of different architecture [20].

Table 2. Characteristics of HTMs used for PSC

Compounds name or abbreviation	HTM	V_{oc} , V	J_{sc} , mA/cm ²	FF, %	PCE, %.	Reference
Spiro-MeOTAD		1.08	21.26	75	16,6-20,2	[14]
P3HT		0.62	14.00	72.2	6.30	[20]
PDPPDBTE		0.85	14.40	74.9	9.20	[20]
TFB		0.96	17.50	0.65	10.92	[21]

PBDTTT-C		0.87	17.68	0.65	9.95	[22]
RCP*		1.08	21.90	0.75	17.30	[23]
PTAA		1.10	17.92	0.54	10.72	[24]
V841		0.91	15.60	0.56	7.96	[24]
V842		0.90	19.49	0.58	10.12	[24]
V873		1.05	19.23	0.61	12.29	[24]



*

Best hole conducting polymers (HCPs), that were synthesized (or newly adapted) for PSC throughout the years can be seen in **Table 2**. One of the first polymer designed solely for perovskite devices was poly[2,5-bis(2-decyldodecyl)pyrrolo[3,4-c]pyrrole-1,4(2H,5H)-dione-(E)-1,2-di(2,2'-bithiophen-5-yl)ethene (PDPPDBTE). This molecule was inspired by donor- π -acceptor materials, that are being used in DSSC. The compound itself, at the time, proved to be an adversary to spiro-MeOTAD, exhibiting efficiency of 9.2% after doping [20].

A class of compounds known as polyfluorenes (PFs) are being widely used in optoelectronics such as: light emitting diodes, field effect transistors, and polymer solar cells

[25]. In the study made by Z. Zhu *et al.*, introduction of electron rich N-triphenyl groups was used to tune the energy levels of monomers, out of which PF compounds were obtained [21]. The best material out of the batch was (poly [(9,9-dioctylfluorenyl-2,7-diyl)-co-(4,4'-(N-(4-sec-butylphenyl)diphenylamine))] (TFB) with which the device exhibited almost 11% after chemical oxidation with LiTFSI in an oxygen atmosphere and 4-tert-butylpyridine (TBP).

Despite the attempts to improve efficiency by the rapid development of different types of device structures, the evolution of HTM is relatively limited. Furthermore, the addition of hygroscopic dopants tends to degrade the perovskite layer, thus shortening the life time of the device [13]. This issue prompted creation of the materials like PBDTTT-C (poly[(4,8-bis-(2-ethylhexyloxy)-benzo[1,2-b:4,5-b']dithiophene)-2,6-diyl-alt-(4-(2-ethylhexanoyl)-thieno[3,4-b]thiophene)-2,6-diyl]) which do not need any dopant at all [22].

Till this day the best polymeric dopant-free material exhibiting the highest efficiency is RCP. It's a copolymer, based on benzo[1,2-b:4,5-b']dithiophene and 2,1,3-benzothiadiazole moiety building blocks. Besides its high efficiency, RCP can form thin films, giving it an advantage over small-molecule HTM that mostly require thicker layers [26;27]. Regardless of this good performance, RCP usage for commercial applications is doubtful, due to its high cost and complicated synthesis.

PTAA (Poly[bis(4-phenyl)(2,4,6-trimethylphenyl)amine]) is one of the best performing polymers used in PSC. It can reach efficiencies up to 20% while doped [26] and 10.72% pristine [24]. Despite its outstanding performance as a HCP, PTAA suffers from the same problems as spiro-MeOTAD: difficult synthesis (in this case obtaining a constant molecular weight (M.W.) every time), high cost and requirement of additives in order to reach high efficiency.

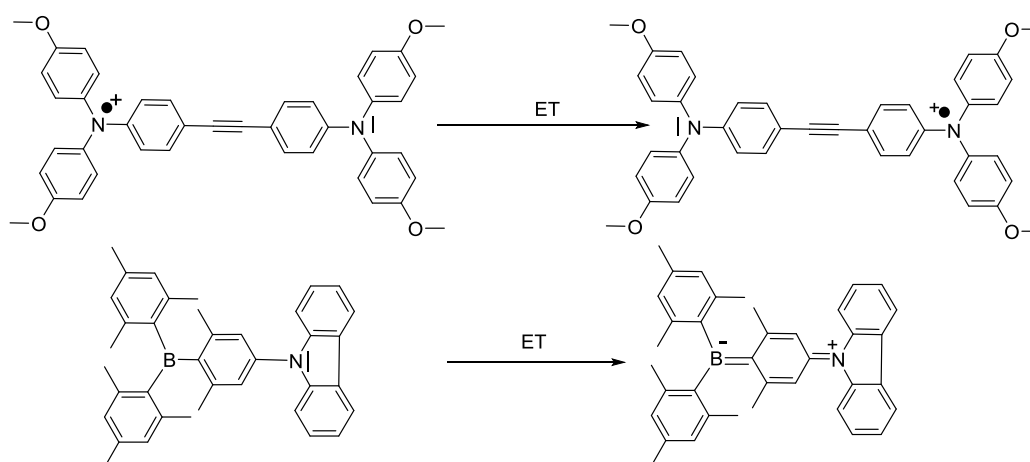
A better alternative is provided by T. Matsui *et al.* [24], they have reported three new HCPs that don't require any additives and can form films as thin as 20 nm. The molecules were based on previously mentioned PTAA. Polymers described in the aforementioned article are used in perovskite solar devices without any additives, that is particularly detrimental for PSC stability. Polymer V873, containing poly[bis(4-phenyl)-(3,5-dimethylphenyl)amine] main chain with methylphenylethenyl fragments attached to it, demonstrates PCE of 12.3% without any additives, which is better than the widely used PTAA [24].

All above mentioned additive-free polymers enhance stability of PSCs and most of them can form good quality films. The greatest challenge of any pristine polymeric hole transporting material (not considering the cost) lies in the reproducibility of the polymer with a constant M.W., thus requiring very controlled synthesis procedures.

2.6 Organic mixed-valence and quaternary ammonium compounds

As stated in chapter 2.3, after the introduction of additives to spiro-MeOTAD, it partially oxidizes, thus becoming more conductive, leading to an idea of developing a compound that already has positive and/or negative charge in its structure, therefore, skipping the doping stage. One of the ways to do it is the use of organic mixed-valence (MV) compounds or materials similar to them.

MV compounds are hard to distinguish from their donor-acceptor (D-A) counterparts. To make things clearer we must consider the similarities of these two classes of systems: both consist of two or more redox centres, with one acting as an electron donor and the other one as an electron acceptor. In both MV and D-A compounds an electron (ET) or charge transfer (CT) can take place between the donor and acceptor moieties (this charge transfer can be induced optically) [28]. The only distinguishing feature is that D-A systems are closed-shell systems, organic MV compounds are always open-shell systems (a valence shell which is not completely filled with electrons) in the ground state (**Scheme 4**). In a sense organic mixed-valence compounds is a subclass of D-A materials, just with a different electron shell system.

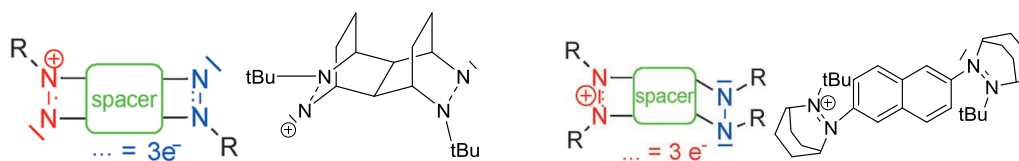


Scheme 4. MV compound (top) compared to D-A material (bottom) upon excitation.

Organic MV systems received interest for their ability to mimic complex ET reactions in nature (e.g. photosynthesis) and also are used in optoelectronics. They are classified on the basis of the functional groups that acts as the redox centers. This classification differs from the one that is being used in inorganic MV system, as in organic structures the charge never solely resides on a single atomic center (like in inorganic) but is delocalized over more than one atom.

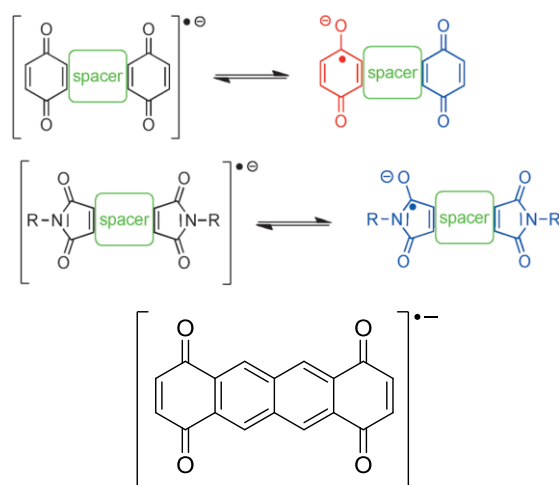
Here are few examples of the most widely studied MV systems. Bis(hydrazyl) and bis(hydrazine) radical-cation systems represent two important classes of organic MV compounds. Although they were not the first systems that were investigated in terms of their mixed valence, they are probably the most intensely studied organic MV materials [28]. In

Scheme 5 we can see the basic structure of both systems, where spacer represents either a saturated bridge or an aromatic one.



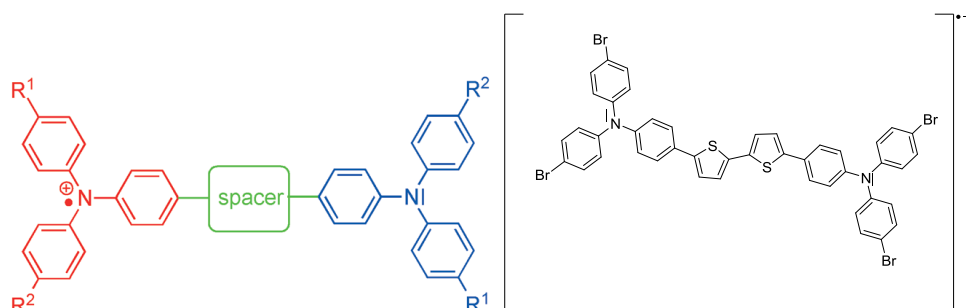
Scheme 5. Bis(hydrazyl) with unsaturated (left) and bis(hydrazine) with an aromatic bridge (right)

Quinones are an important class of organic redox system that is widely used both in nature as redox coenzymes and in synthesis as oxidizing reagents. In **Scheme 6** the spacer in quinones is an unsaturated group of atoms.



Scheme 6. Basic quinone structures

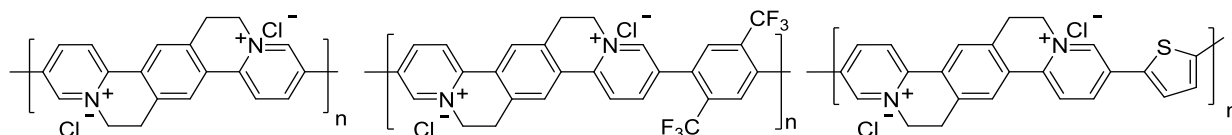
Bis(triarylamine) radical cations demonstrate excellent properties which promote a detailed optical investigation of their ET behavior. Furthermore, they are widely used as hole-transport components in photoconductors and light-emitting devices and thus, were one of the first types of organic MV compounds with possible practical applications. The spacer in **Scheme 7** represents unsaturated group of atoms [28].



Scheme 7. Bis(triarylamine) radical cation

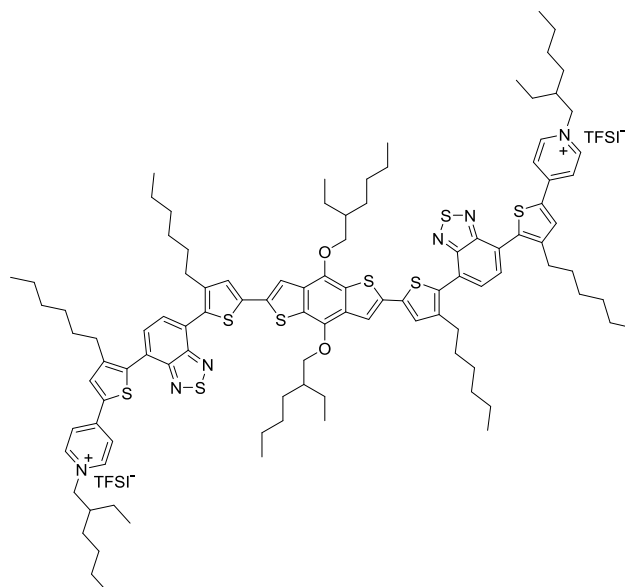
Polymers containing pyridinium derivatives in their structure incorporate the idea of having a charge in a molecule. The formation of pyridinium salts is possible due to a pair of unpaired electrons of the nitrogen atom in the pyridine ring. Resulting in a charge formation

within the structure, with counter ion (like chlorine) to stabilize the structure. An example of such a framework is shown in **Scheme 8**, where pyridine fragment is incorporated into polymeric ETMs. These derivatives are soluble only in highly polar solvents such as methanol and water, which allows for the facile formation of multilayer polymer structures by simple deposition techniques. [29].



Scheme 8. Quaternary amino ETMs [29]

After the emergence of quaternary ammonium ETMs, additive free ionic type HTMs that are based on 2-ethylhexyloxy substituted benzodithiophene (BDT) core unit were reported [30]. Similarly to HTM X44 mentioned in chapter 2.4 the compounds incorporated ionized pyridine units that were stabilized by TFSI⁻ anions. Applied in PSCs, ionic molecular material coded as M7-TFSI exhibited efficiency of 17.4% (**Scheme 9**). These results can be attributed to a deep highest occupied molecular orbital (HOMO) energy level, high hole mobility and high conductivity of M7-TFSI. Unsurprisingly the absence of additives prolonged the lifetime of PSCs tested with the above-mentioned compound, but the lengthy synthesis and expensive precursors makes it hardly suitable for commercial applications.



Scheme 9. HTM M7-TFSI [30]

In general, there are not that many HTMs for PSC applications with ionic moieties synthesised till this day. Therefore, further research is required about the applications of these compounds in perovskite devices.

2.7 Literature review conclusions

Upon having studied the relevant literature a few conclusions can be made:

- In PSC devices a cheaper, but similarly efficient alternative for spiro-MeOTAD is required.
- Additive free HTMs enhance the stability of PSCs without a significant loss in efficiency compared with devices that use doped spiro-MeOTAD as a hole injecting layer.
- Perovskite solar cells characteristics are more reproducible with low molecular weight additive-free compounds than with polymeric charge transporting materials due to the difficulty of synthesising polymers with a constant M.W.
- Addition of ions tends to increase the conductivity of a HTM
- Ionic HTMs, incorporating counter ions (particularly TFSI) for stabilizing quaternary ammonium groups, exhibit efficiencies of more than 15%.

All of the aforementioned conclusions and the lack of studies of ionic HTMs suitable for PSC encourage us to synthesis and study properties of ionic compounds for application as HTM in PSC.

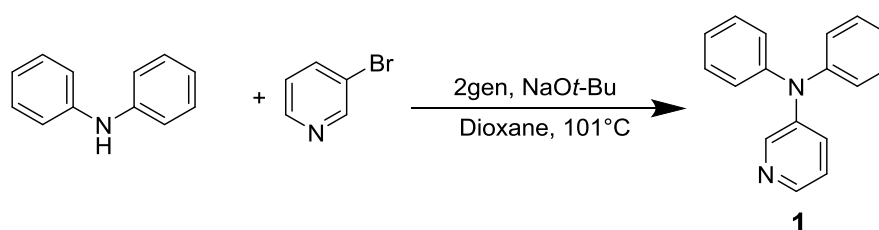
3. Results and discussion

These days in the field of optoelectronics chemists and material scientists alike are faced with a task to create compounds that are long-lasting, cheap, easily produced. Therefore, synthesis of organic semiconductors that fit all the above-mentioned criteria is one of the highest priority.

Most of the materials now used in photovoltaics require dopants that lower the general stability of the fabricated perovskite device. A solution to this problem could be organic quaternary salts that are inexpensive and do not need any additives at all. For this cause TPA based ionic compounds and pyridine derivative containing materials were synthesized and investigated as HTMs.

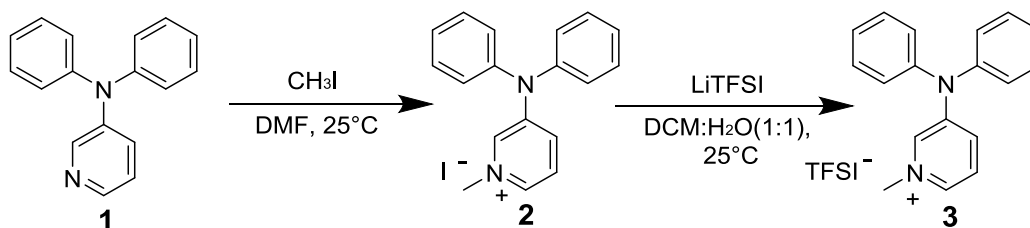
3.1 Synthesis of model compounds

Before synthesizing the aforementioned ionic HTMs a synthesis of model compounds was conducted. The first step was the Buchwald-Hartwig coupling reaction: diphenylamine and 3-bromopyridine were coupled in anhydrous dioxane under argon atmosphere in the presence of base sodium tertbutoxide and second generation palladium precatalyst giving *N,N*-diphenylpyridin **1** as a product (**Scheme 10**).



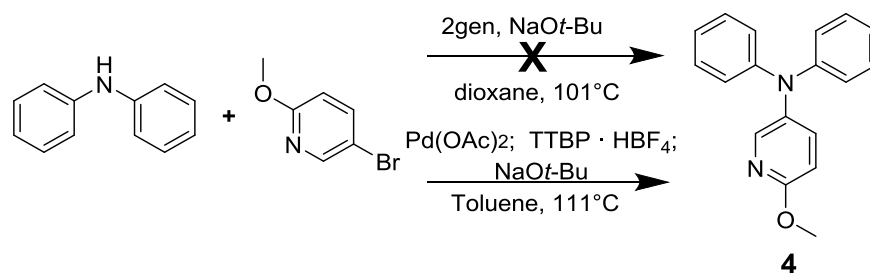
Scheme 10. Synthesis of *N,N*-diphenylpyridin-3-amine (**1**)

3-(diphenylamino)-1-methylpyridin-1-ium iodide (**2**) was synthesized by the reaction of **1** and methyl iodide in anhydrous DMF. The change of iodine anion to TFSI is necessary for the stability of PSC (iodine ion is small and can travel to other layers of the device thus potentially lowering the efficiency and stability of the device). LiTFSI and **2** reacted in a mixture of DCM and H₂O (1:1) giving 3-(diphenylamino)-1-methylpyridin-1-ium bis(trifluoromethanesulfonyl)azanide (**3**).



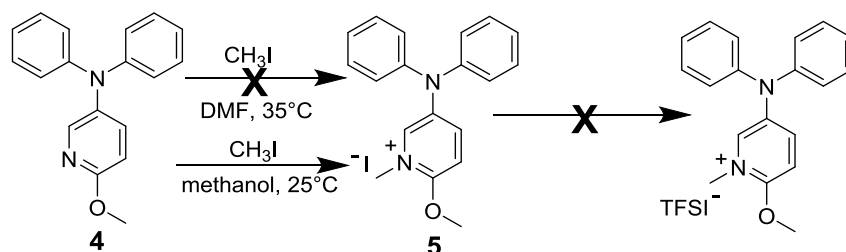
Scheme 11. Synthesis of ionic moieties **2** and **3**

The addition of methoxy groups tends to lower I_p due to their donor properties, therefore a methoxy group containing analogue 6-methoxy-*N,N*-diphenylpyridin-3-amine (**4**) was synthesised, however the first attempt on acquiring **4** might have failed due to the poor choice of a catalytic system and/or the unsuitable polarity of the solvent. The reaction was carried out successfully using the Buchwald-Hartwig coupling reaction between diphenylamine and 5-bromo-2-methoxypyridine in anhydrous toluene under argon atmosphere using palladium (II) acetate, tri-*tert*-butylphosphonium tetrafluoroborate as a catalytic system and sodium *tert*butoxide as a base (**Scheme 12**).



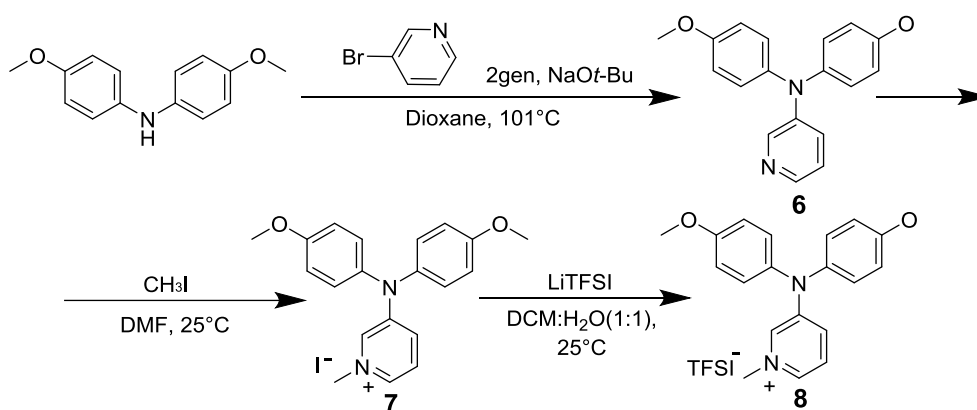
Scheme 12. Synthesis of 6-methoxy-*N,N*-diphenylpyridin-3-amine (**4**)

5-(diphenylamino)-2-methoxy-1-methylpyridin-1-ium iodide (**5**) was synthesized by the reaction of **4** and methyl iodide in methanol. The reaction could not have been conducted the usual way - using DMF as solvent, probably due to the reaction occurring between DMF and **4** or a side reaction between the reactants. The yield of aforementioned reaction was very low, therefore the change of I⁻ anion to TFSI⁻ could not be conducted (**Scheme 13**).



Scheme 13. Synthesis of 5-(diphenylamino)-2-methoxy-1-methylpyridin-1-ium iodide (**5**)

After the unsuccessful attempt of changing iodine anion to TFSI⁻ in compound **5**, a decision was made to change the placement of the methoxy groups in hope to get a full range of model compounds in high yields (**Scheme 14**).



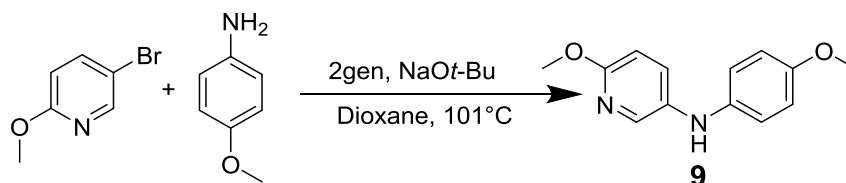
Scheme 14. Synthesis of *N,N*-bis(4-methoxyphenyl)pyridin-3-amine **6** and its ionic moieties (**7**),
(**8**)

Synthesis of *N,N*-bis(4-methoxyphenyl)pyridin-3-amine (**6**), 3-[bis(4-methoxyphenyl)amino]-1-methylpyridin-1-ium iodide (**7**) and 3-[bis(4-methoxyphenyl)amino]-1-methylpyridin-1-ium bis(trifluoromethanesulfonyl)azanide (**8**) were conducted similarly to materials **1**, **2** and **3**. Compound **6** was synthesized by coupling 3-bromopyridine and 4,4'-dimethoxydiphenylamine in anhydrous dioxane under argon atmosphere using second generation palladium precatalyst and sodium tertbutoxide as base. After purification, the acquired compound and methyl iodide were reacted in anhydrous DMF giving **7** as product, which in the next step of synthesis was dissolved together with LiTFSI in a mixture of DCM and H₂O (1:1) to obtain ionic compound **8**.

3.2 Synthesis of pyridine containing Spiro-MeOTAD and V886 derivatives

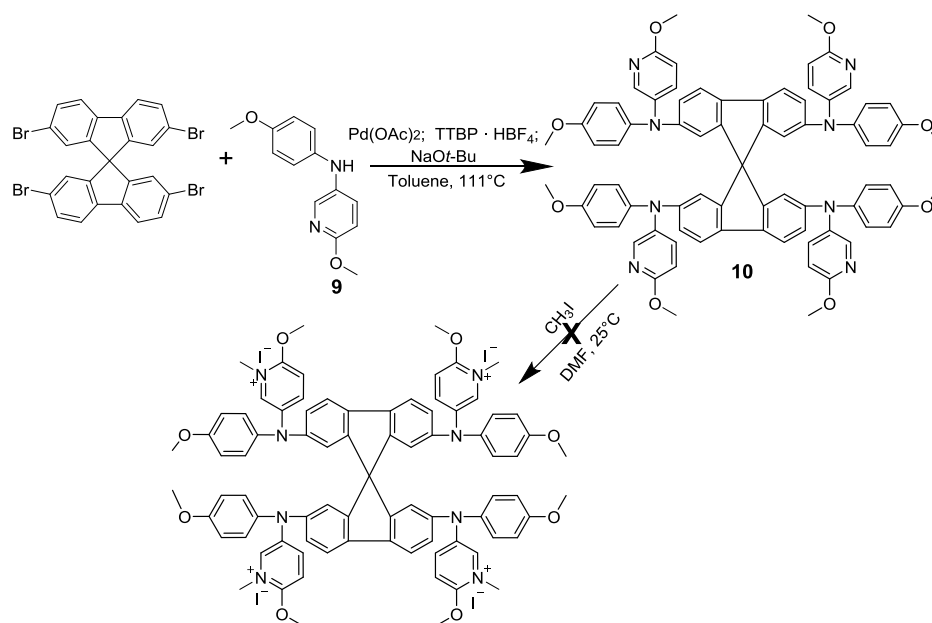
To observe the change of properties on a bigger scale, it was decided to introduce pyridine moieties to well-known HTMs - spiro-MeOTAD and V886, with the final goal in mind being quaternary salts of the aforementioned compounds.

To achieve this objective 6-methoxy-*N*-(4-methoxyphenyl)pyridin-3-amine (**9**) was synthesised using Buchwald-Hartwig coupling reaction. 5-bromo-2-methoxypyridine and *p*-anisidine were dissolved in anhydrous dioxane under argon atmosphere, afterwards second-generation palladium precatalyst and sodium tertbutoxide were added to the mixture to obtain **9** as product (**Scheme 15**)



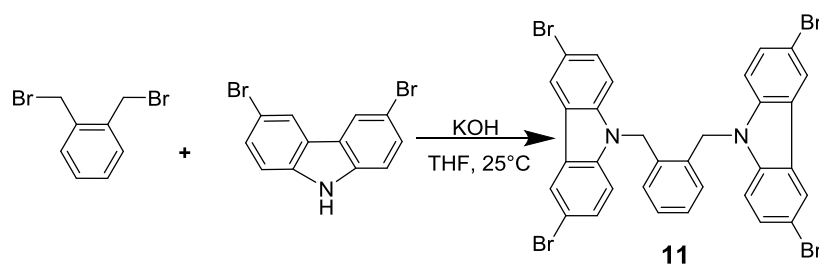
Scheme 15. Synthesis of 6-methoxy-*N*-(4-methoxyphenyl)pyridin-3-amine (**9**)

Amine **9** was used in a reaction with 2,2',7,7'-Tetrabromo-9,9'-spirobi[9H-fluorene] in an anhydrous toluene under argon and in the presence of palladium (II) acetate, tri-tert-butylphosphonium tetrafluoroborate and sodium tertbutoxide to yield N^2, N^2', N^7, N^7' -tetrakis(4-methoxyphenyl)- N^2, N^2', N^7, N^7' -tetrakis(6-methoxypyridin-3-yl)-9,9'-spirobi[fluorene]-2,2',7,7'-tetramine (**10**). The acquired compound **10** was then used in a reaction with methyl iodide in an attempt to synthesise an ionic moiety of the aforementioned HTM, however the desired product could not be obtained due to the difficulties in purification (**Scheme 16**).



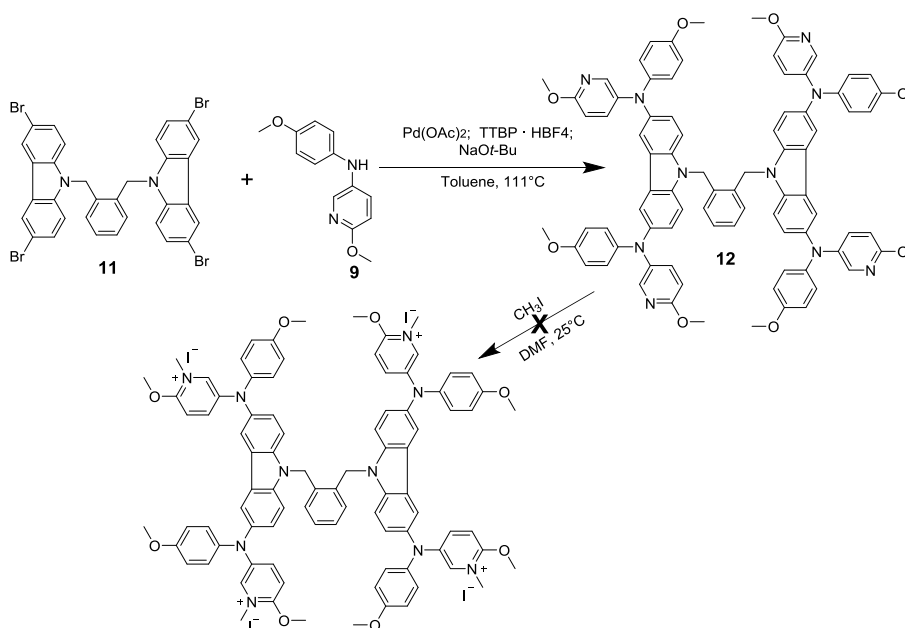
Scheme 16. Synthesis of spiro-MeOTAD derivative **10** and its ionic moiety

To obtain HTM **12** a 9,9'-[1,2-phenylenebis(methylene)]bis(3,6-dibromo-9H-carbazole) (**11**) was acquired by condensation of 1,2-bis(bromomethyl)benzene and 3,6-dibromocarbazole in THF, in the presence of potassium hydroxide (**Scheme 17**).



Scheme 17. Synthesis of 9,9'-[1,2-phenylenebis(methylene)]bis(3,6-dibromo-9H-carbazole) (**11**)

Carbazole derivative **11** was used in a reaction with amine **9** in an anhydrous toluene under argon, in the presence of palladium (II) acetate, tri-tert-butylphosphonium tetrafluoroborate and sodium tertbutoxide to obtain 9,9'-[1,2-phenylenebis(methylene)]bis[N^3, N^6 -bis(4-methoxyphenyl)- N^3, N^6 -bis(6-methoxypyridin-3-yl)-9H-carbazole-3,6-diamine] (**12**).

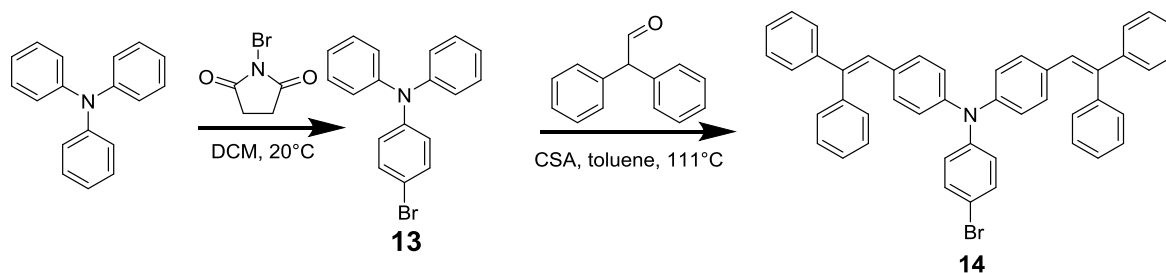


Scheme 18. Synthesis of V886 derivative **12** and its ionic moiety

The acquired compound **12** was then used in a reaction with methyl iodide in an attempt to synthesise an ionic moiety of the aforementioned HTM. The obtained amorphous mass could not be purified by any conventional purification method, therefore further experiments were not conducted neither with HTM **12** nor **10** (**Scheme 18**).

3.3 Synthesis of triphenylamine based ionic hole transporting materials

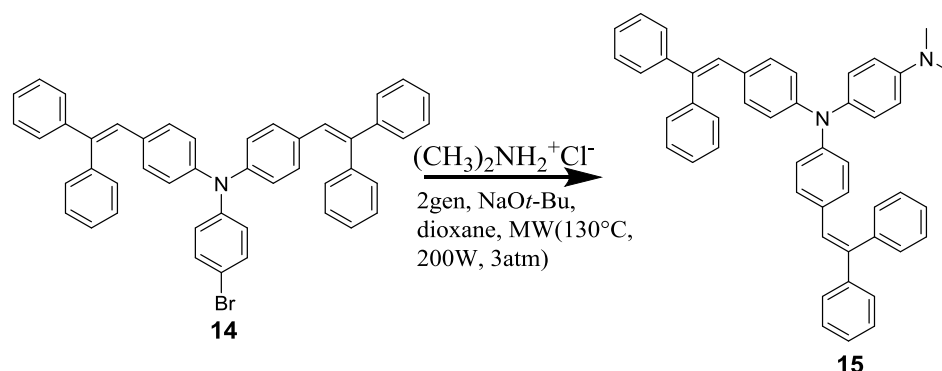
After the failed attempts to obtain ionic HTMs based on spiro-MeOTAD and V886 it was decided to synthesise triphenylamine (TPA) based quaternary ammonium salts. 4-bromo-*N,N*-diphenylaniline (**13**) was acquired *via* bromination of TPA in DCM. The acquired product was used in a condensation reaction with diphenylacetaldehyde in toluene in the presence of camphor-10-sulfonic acid (β) (CSA) yielding 4-bromo-*N,N*-bis[4-(2,2-diphenylethenyl)phenyl]aniline (**14**) (**Scheme 19**).



Scheme 19. Synthesis of 4-bromo-*N,N*-diphenylaniline (**13**) and 4-bromo-*N,N*-bis[4-(2,2-diphenylethenyl)phenyl]aniline (**14**)

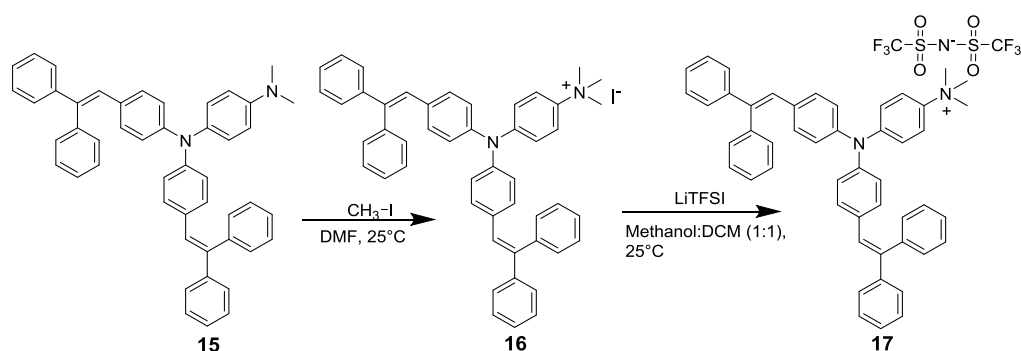
Triphenylamine **14** and dimethyl amine hydrochloride were used in a microwave assisted Buchwald-Hartwig coupling reaction under argon in anhydrous dioxane (**Scheme 20**), under

pressure and elevated temperature giving N^l, N^l -bis[4-(2,2-diphenylethenyl)phenyl]- N^d, N^d -dimethylbenzene-1,4-diamine (**15**) as product.



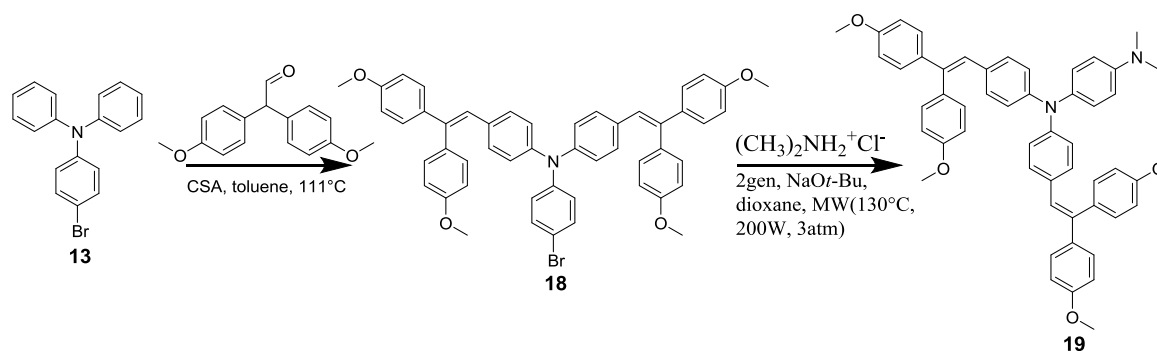
Scheme 20. Synthesis of N^l, N^l -bis[4-(2,2-diphenylethenyl)phenyl]- N^d, N^d -dimethylbenzene-1,4-diamine (**15**)

4-{bis[4-(2,2-diphenylethenyl)phenyl]amino}- N, N, N -trimethylanilinium iodide (**16**) was obtained by the addition reaction between amine **15** and methyl iodide in anhydrous DMF. Similarly to the model compounds, the iodine ion in quaternary ammonium salt **16** was changed to TFSI ion by the addition of LiTFSI to a solution of **16** in DCM and H_2O (1:1), yielding 4-{bis[4-(2,2-diphenylethenyl)phenyl]amino}- N, N, N -trimethylanilinium bis(trifluoromethanesulfonyl)azanide (**17**) (**Scheme 21**).



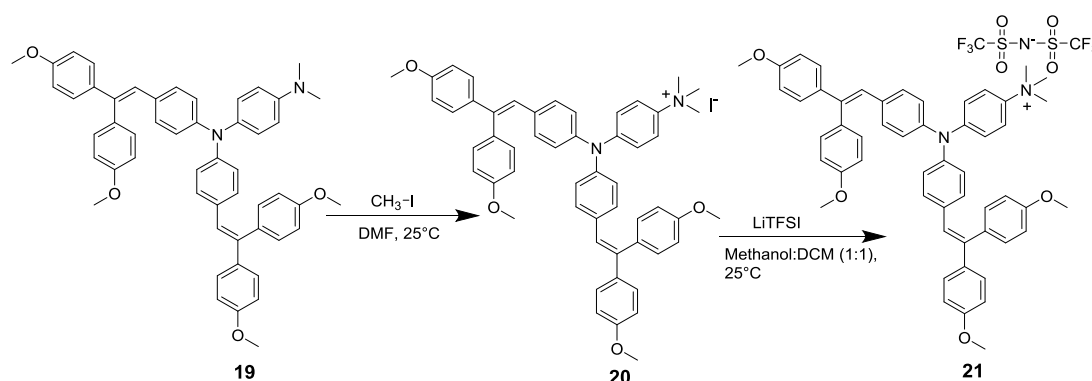
Scheme 21. Synthesis of ionic moieties **16** and **17**

Using previously acquired 4-bromo- N, N -diphenylaniline (**13**) a condensation reaction with 2,2-bis(4-methoxyphenyl)acetaldehyde was conducted in toluene using CSA as a catalyst. The obtained product - 4-[2,2-bis(4-methoxyphenyl)ethenyl]- N -{4-[2,2-bis(4-methoxyphenyl)ethenyl]phenyl}- N -(4-bromophenyl)aniline (**18**) was used to synthesis N^l, N^l -bis{4-[2,2-bis(4-methoxyphenyl)ethenyl]phenyl}- N^d, N^d -dimethylbenzene-1,4-diamine (**19**) by microwave assisted Buchwald-Hartwig coupling reaction (**Scheme 22**).



Scheme 22. Synthesis of brominated compound **18** and its derivative **19**

Amine **19** was used to synthesis 4-(bis{4-[2,2-bis(4-methoxyphenyl)ethenyl]phenyl}amino)-*N,N,N*-trimethylanilinium iodide (**20**) by the addition of methyl iodide to a solution of **19** in anhydrous DMF.



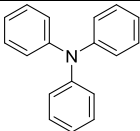
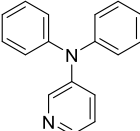
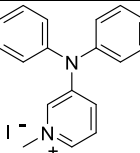
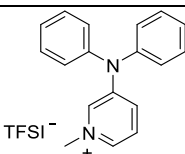
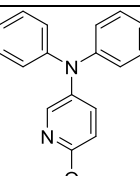
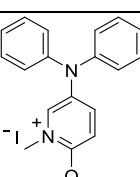
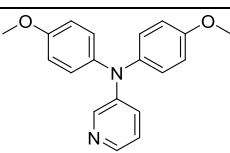
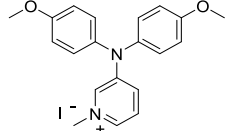
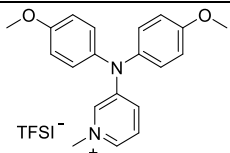
Scheme 23. Synthesis of ionic moieties **20** and **21**

The acquired product **20** was then dissolved together with LiTFSI in a mixture of DCM and methanol (1:1) yielding 4-(bis{4-[2,2-bis(4-methoxyphenyl)ethenyl]phenyl}amino)-*N,N,N*-trimethylanilinium bis(trifluoromethanesulfonyl)azanide (**21**) (**Scheme 23**).

3.4 Thermal properties of synthesized materials

One of the basic requirements for optoelectronic device fabrication is the ability to form good quality amorphous films. For this purpose, organic semiconductors must have high T_g . In this work, we have synthesized a group of model compounds (**1-8**) that were used to observe the variation of thermal properties due to the change in the molecular structure of a HTM (**Table 3**). T_g and melting point (T_m) were determined using differential scanning calorimetry.

Table 3. T_g and melting temperatures of model compounds

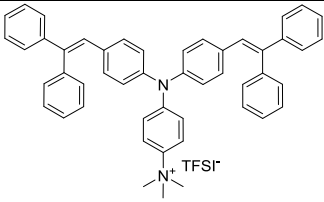
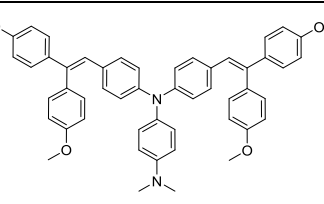
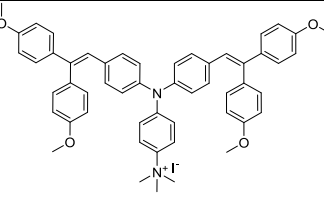
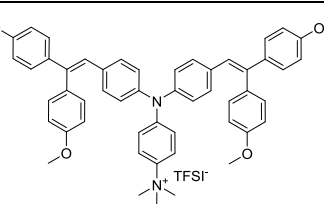
Compound	Structure	T_g , C°	T_m , C°
TPA		-	127
1		-	99
2		40	201
3		-13	75
4		-9	65
5		25	134
6		-9	-
7		6	-
8		-9	-

After analyzing the results presented in **Table 3** a few observations were made: the change of phenyl group to a pyridine ring lowers T_m , introduction of iodine anion leads to an increase in T_g and/or the increase in T_m ; the change of iodine to TFSI anion lowers T_g and/or T_m .

After the investigation of thermal properties of the acquired model compounds, the optimal pyridine fragment was selected and HTMs **10**, **12** were synthesised. **Table 4** gives an overview of the thermal properties of aforementioned positive charge transporting materials.

Table 4. T_g and melting temperatures of HTMs

Compound	Structure	T_g , C°	T_m , C°
10		115	228
Spiro-MeOTAD		124	246
12		138	225
V886		141	-
15		63	-
16		-	146

17		85	-
19		88	-
20		86	129
21		83	-

After analyzing the results of **Table 4** these observations were made: in case of HTMs **10** and **12** the change of phenyl group to a pyridine fragment lowers somewhat the T_g and T_m ; the introduction of iodine anion leads to a formation of a crystalline (**16**) or partially crystalline (**20**) state; the change from iodine anion to TFSI leads to a change from crystalline (or partially crystalline) to amorphous state; Adding methoxy groups has practically no effect on the T_g and T_m of ionic compounds (**16**, **17** and **20**, **21**), but significantly increases the T_g of HTM **19**.

3.5 Optical properties of synthesized materials

Organic semiconductor's UV-vis absorption spectrum can provide important information about the investigated HTMs. From it we can determine the size of the conjugated π -electron system. Knowledge of the relative size of the conjugated system helps to predict the charge transport efficiency in an optoelectronic device.

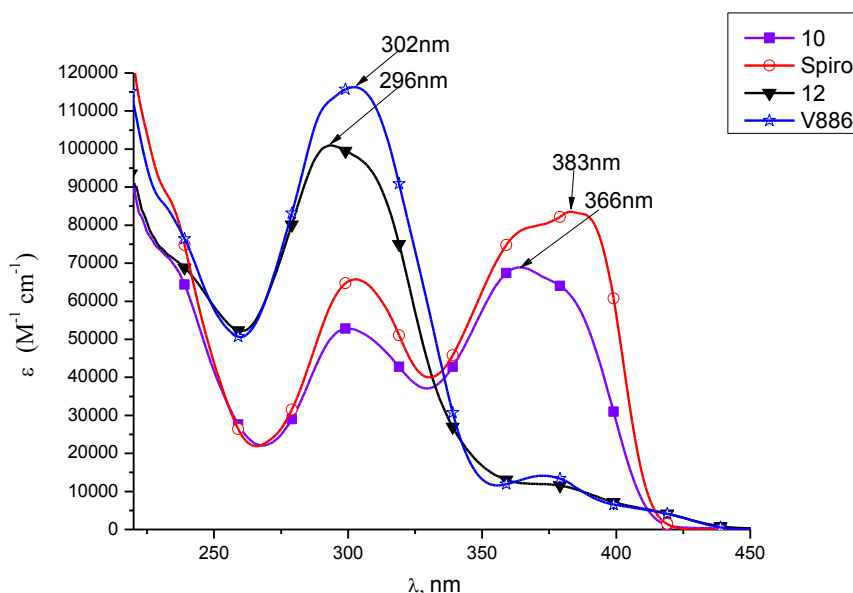


Figure 4. UV-vis absorption spectra of **10**, **12**, spiro-MeOTAD and V886

UV-vis absorption spectra of spiro-MeOTAD, V886 and their investigated derivatives HTMs **10** and **12** respectively, can be seen in **Figure 4**. The obtained results suggest that the addition of pyridine moieties barely changes the size of the conjugated system, however compounds with heterocyclic rings exhibits a hypochromic effect, assumedly due to the change in their spatial structure compared to the above mentioned spiro-MeOTAD and V886.

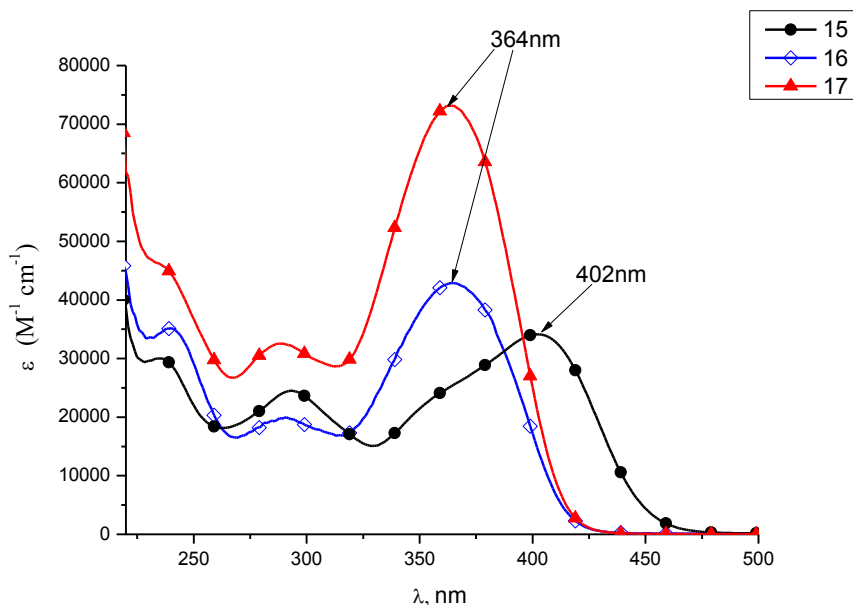


Figure 5. UV-vis absorption spectra of investigated compounds **15**, **16**, **17**

After the introduction of ionic group to a compound such as N^l, N^l -bis[4-(2,2-diphenylethenyl)phenyl]- N^d, N^d -dimethylbenzene-1,4-diamine (**15**) a hypsochromic shift occurs (**Figure 5**). This alteration demonstrates the decrease of electron density in the conjugated system due to the formation of ionic derivatives. However, compared to HTM **15** a

hyperchromic effect for ionic moieties **16** and **17** is observed as well. This could be explained by the change in the electron distribution within the molecule.

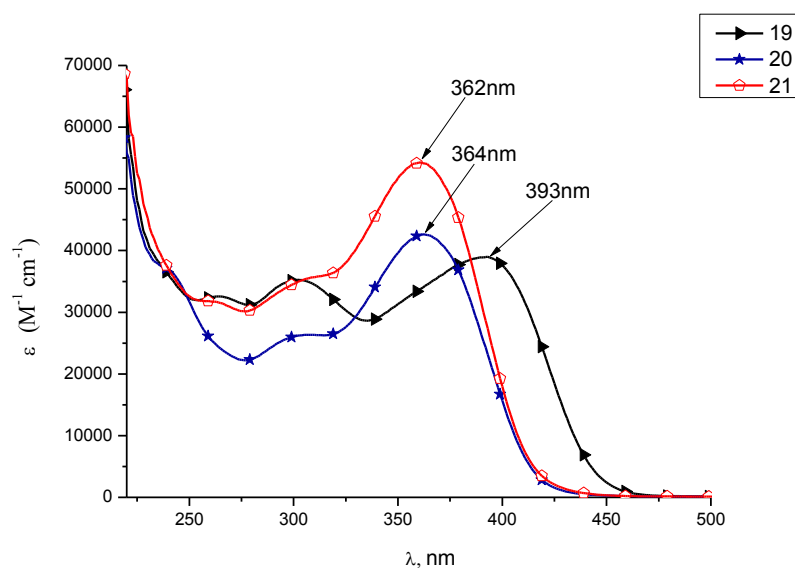


Figure 6. UV-vis absorption spectra of HTMs **19**, **20**, **21**

Similar tendencies to previously mentioned group of HTMs (**15-17**) are seen for HTMs **19-21** (**Figure 6**). The hyperchromic effect in compounds **20** and **21** as well as their hypsochromic shift compared to N^l, N^l -bis{4-[2,2-bis(4-methoxyphenyl)ethenyl]phenyl}- N^d, N^d -dimethylbenzene-1,4-diamine (**19**) is evident. However, an unusual result can be noticed after analysing the data of both **Figure 5** and **Figure 6**: the addition of methoxy donor groups in HTMs **19-21** (**Figure 6**) does not produce an expected bathochromic shift when compared to the UV-vis absorption spectra of compounds **15-17**. Such outcome can be attributed to some steric hindrances in the spatial structure of the previously mentioned HTMs due to the added methoxy groups.

3.6 Photoelectric properties of investigated materials

Energy level compatibility of different layers is a necessity for any efficient optoelectronic device. The easiest way to predict it is with the measurement of I_p . For PSC application, the desired I_p of a HTM is in the range from 5.0eV to 5.4eV.

Table 4. I_p results of investigated compounds¹

Compound number	I_p
1	5.20
2	5.45
3	5.90
4	5.47

¹ Measurements were carried out at the department of solid state electronics, Vilnius University.

5	5.69
6	5.60
7	-
8	5.75
10	5.26
12	5.24
15	5.30
16	5.46
17	5.80
19	5.10
20	5.41
21	5.45

Before synthesizing HTMs **10-21** examination of model materials ionization potential was carried out. After analyzing the acquired I_p results of compounds **1-8** (Table 4) a few conclusions can be made: the I_p of materials **1**, **4**, and **6** rises depending on the amount of methoxy groups in a compound; addition of iodine ions leads to an increase in I_p ; the change from iodine anion to a TFSI tend to increase the I_p ; TFSI anion containing material **3** has a higher I_p compared to the methoxy groups possessing analogue **8**.

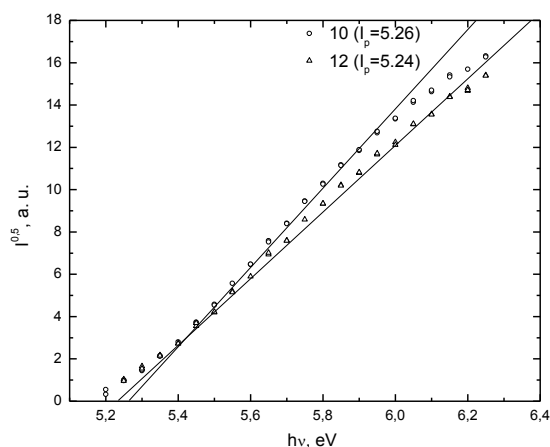


Figure 7. I_p measurements of investigate compounds **10** and **12**.

As mentioned before, HTMs **10** and **12** were based on well-known compounds spiro-MeOTAD and V886 respectively, with the key difference between them being pyridine derivatives in the molecular structure of the foremost. The change of phenylenes to heterocyclic moieties in **10** and **12** leads to an increase of I_p compared to spiro-MeOTAD ($I_p=5.0\text{eV}$ [14]) and V886 ($I_p=5.04$ [33]) (Figure 7), suggesting that pyridine derivatives weaken the donoric properties of the investigated materials **10** and **12**.

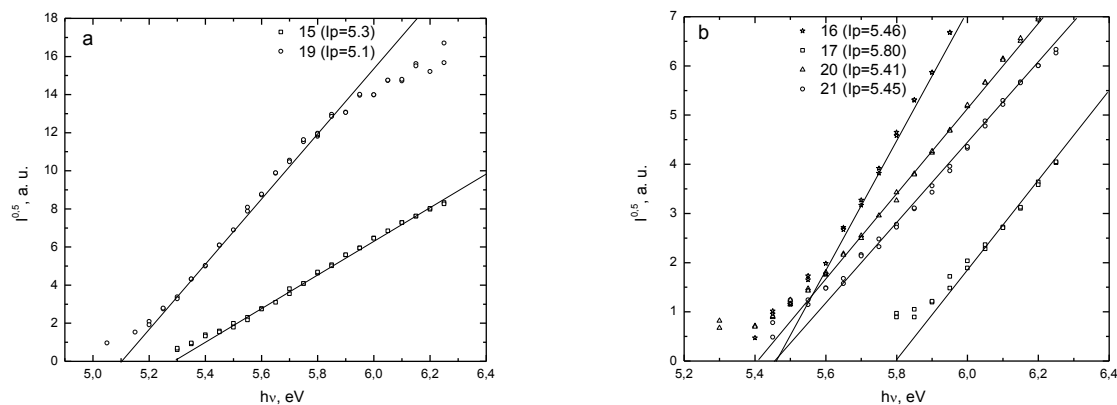


Figure 8. I_p measurements of HTMs **15**, **19** (a) and their ionic moieties **16**, **17**, **20**, **21** (b).

The effect of the addition of donoric methoxy groups can be seen in both graphs of **Figure 8**: all alkoxy group containing materials (**19**, **20**, **21**) have lower I_p compared to their respective analogues (**15**, **16**, **17**). Furthermore, **Figure 8** provides a view on the impact of I_p after the introduction of ionic moieties. The increase of energy needed to excite an electron from HOMO to LUMO in ionic compounds could be explained by the decrease of the amino group donoric properties after the formation of quaternary ammonium moiety.

One of the main goals of this work was to test the synthesized HTMs in PSCs. HTMs **10**, **12**, **15** and **19** were used with additives in the fabrication of perovskite solar cells while **16**, **17**, **20**, **21** were used pristine. The results of characterization of the devices are shown in the **Table 5**. The presented values are as follows: σ conductivity of a HTM, open circuit voltage (V_{oc}) short circuit current (J_{sc}), fill factor (FF) and power conversion efficiency (PCE).

Table 5. Parameters of PSC devices fabricated using investigated HTMs²

Compound number	σ , S/m	V_{oc} , V	J_{sc} , mA/cm ²	FF , %	PCE , %.
10	-	-	-	-	2.9
12	-	-	-	-	0.0
15	$5 \cdot 10^{-10}$	0.79	12.3	34	3.5
16	$1.7 \cdot 10^{-9}$	0.51	1.2	41	0.3
17	$6 \cdot 10^{-9}$	0.24	0.0	21	0.0
19	$1 \cdot 10^{-9}$	-	-	-	3.5
20	$0.7 \cdot 10^{-9}$	-	-	-	0.3
21	$0.7 \cdot 10^{-9}$	-	-	-	0.0

The best performing devices were fabricated using doped HTMs **10**, **15** and **19** (PCE : 2.9%, 3.5%, 3.5% respectively), material **12** and additive free ionic moieties **16**, **17**, **20**, **21** displayed none or very low efficiency. Such low performance of quaternary ammonium

²Conductivity measurements were carried out at the department of solid state electronics, Vilnius University, while the devices were fabricated and tested at EPFL Institute of Chemical Sciences and Engineering.

compounds can be attributed to their low conductivity while the spatial structure of doped HTMs together with their unfavourable photoelectric properties could have also lead to poor performance.

4. Experimental details

4.1 General Methods and Materials

Chemicals were purchased from Sigma-Aldrich and TCI Europe and used as received without further purification. *N,N*-diphenylpyridin-3-amine **1** was synthesized according to an earlier reported procedure [31]. Synthesis of compounds **15** and **19** were conducted in CEM Discover Synthesis Unit (CEM Corp., Matthews NC) microwave reactor. The course of the reactions was monitored by TLC (thin layer chromatography) on ALUGRAM SIL G/UV254 plates and developed with I₂ or UV light. Silica gel (grade 9385, 230–400 mesh, 60 Å, Aldrich) was used for column chromatography. The ¹H and ¹³C NMR spectra were taken on Bruker Avance III 400 (400 MHz) and Bruker Avance III 700 (700 MHz) spectrometers at room temperature. The chemical shifts, expressed in δ (ppm) are relative to a (CH₃)₄Si (TMS, 0 ppm) internal standard. Elemental analysis was performed with an Exeter Analytical CE-440 elemental analyzer, Model 440 C/H/N/. Differential scanning calorimetry (DSC) was performed on a Q10 calorimeter (TA Instruments) at a scan rate of 10 K/min in the nitrogen atmosphere. The glass transition temperatures for the investigated compounds were determined during the second heating scan. Melting point for crystalline materials were observed using Mel-Temp DigiMelt MPA 161 melting point apparatus at a scan rate 1 C°/min. UV/Vis spectra were recorded on a PerkinElmer Lambda 35 spectrometer.

Ionization-potential measurements (*I_p*)

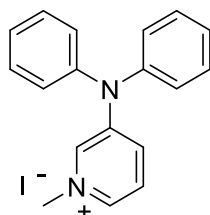
The ionization potential (*I_p*) of the layers of the synthesized compounds was measured by electron photoemission in air. The samples were prepared by dissolution in THF and the solutions were coated on Al plates pre-coated with approximately 0.5 μm thickness of a methyl methacrylate and methacrylic acid copolymer adhesive layer. The thickness of the transporting material layer was 0.5 – 1 μm. The organic materials investigated are stable enough to oxygen that the measurements may be carried out in the presence of air. The samples were illuminated with monochromatic light from a quartz monochromator fitted with a deuterium lamp. The power of the incident light beam was (2–5)·10⁻⁸ W. A negative voltage (-330 V) was supplied to the sample substrate. The counter electrode with a 4.5 · 15 mm² slit for illumination was placed 8 mm from the sample surface. The counter electrode was connected to the input of the BK2–16 type electrometer, working in the open input regime, for the photocurrent measurement. The 10⁻¹⁵ – 10⁻¹² A photocurrent (*I*) flowed in the circuit under illumination. The value of *I* is strongly dependent on the incident-light photon energy (*hν*). The dependence *I*^{0.5} on incident-light quanta energy *hν* was plotted from the experiment results. Usually the dependence of *I* on the incident light quantum energy is described well by the linear relationship *I*^{0.5} = *f*(*hν*) near the threshold.

The linear part of this dependence was extrapolated to the $h\nu$ axis and the I_p value was determined as the photon energy at the interception point.

Perovskite solar cell fabrication and characterization

The solar cells were built on NSG10 glass and a 30-50nm thick TiO_2 blocking layer was produced by spray pyrolysis. The mesoporous TiO_2 (150mg 30NRD Dyesol paste per 1 ml of EtOH) layer was applied by spin-coating for 20 s (5000rpm, 2000rpm/s) and annealed at 500°C for 15 min. 1.1M PbI_2 /MAI (1:1) in DMSO was spin coated using chlorobenzene as an antisolvent. The perovskite layer was deposited inside a Nitrogen glovebox. The hole transporting material was applied by spin-coating for 20 s at 4000 rpm from a chlorobenzene solution (16.1mg in 400 μl , 30mmol) using LiTFSI (3.5 μl from a 520mg/ml stock solution in acetonitrile). Fabrication of the device was completed by evaporation of 90 nm of gold as the counter electrode. The Current–voltage characteristics for all cells were measured with a Keithley 2400 under 1000 W m^{-2} , AM 1.5G conditions (LOT ORIEL 450 W).

4.2 Description of synthesis

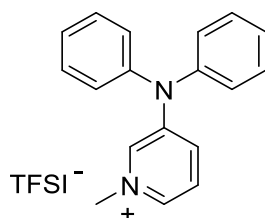


3-(diphenylamino)-1-methylpyridin-1-ium iodide (2): a mixture of *N,N*-diphenylpyridin-3-amine (0.77g, 3mmol) and methyl iodide (0.639g, 4.5mmol) were dissolved in anhydrous DMF (10ml). The reaction was conducted at room temperature for 4 hours. Afterwards the reaction mixture was poured to 100ml of diethyl ether and cooled to -5°C for 1 hour, precipitate was formed and filtrated giving amorphous yellow powder (1.02g, 88%).

Elemental analysis calcd (%) for $\text{C}_{18}\text{H}_{17}\text{IN}_2$ (388.06g/mol): C 55.68, H 4.41, I 32.69, N 7.22; found: C 55.45, H 4.58, N 7.44.

$^1\text{H NMR}$ (700 MHz, CDCl_3 , 25°C , TMS) δ 8.64 (d, $J = 3.4$ Hz, 1H, Ht), 7.83 (s, 1H, Ht), 7.70 (d, $J = 13.4$ Hz, 2H, Ht), 7.46 (t, $J = 7.7$ Hz, 4H, Ph), 7.33 (d, $J = 8.3$ Hz, 6H, Ph), 4.44 (s, 3H, CH_3) ppm.

$^{13}\text{C NMR}$ (176 MHz, CDCl_3 , 25°C , TMS) δ 148.34 (Ht), 143.20 (Ht), 135.51 (Ht), 132.48 (Ht), 130.91, 130.84, 128.02, 127.57, 126.51, 50.31 (CH_3) ppm.

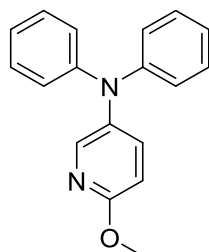


3-(diphenylamino)-1-methylpyridin-1-ium bis(trifluoromethanesulfonyl)azanide (3): a mixture of 3-(diphenylamino)-1-methylpyridin-1-ium iodide (0.5g, 1.13mmol) and (0.74g, 2.6mmol) lithium TFSI were dissolved in DCM (4ml) and distilled H₂O (4ml). The reaction was conducted at room temperature for 23 hours. Afterwards solvent was removed leaving yellow amorphous material, which then was washed with distilled H₂O and dried over vacuum, giving the pure product **3** as yellow powder (0.502g, 88%).

Elemental analysis calcd (%) for C₂₀H₁₇F₆N₃O₄S₂ (246.12g/mol): C 44.36, H 3.16, F 21.05, N 7.76, O 11.82, S 11.84; found: C 44.25, H 3.02, N 7.94.

¹H NMR (700 MHz, CDCl₃, 25°C, TMS) δ 8.03 (d, *J* = 5.7 Hz, 1H, Ht), 7.75 (s, 1H, Ht), 7.70 (dd, *J* = 8.9, 2.0 Hz, 1H, Ht), 7.60 (dd, *J* = 8.9, 5.8 Hz, 1H, Ht), 7.45 (t, *J* = 7.9 Hz, 4H, Ph), 7.32 (t, *J* = 7.5 Hz, 2H, Ph), 7.26 (d, *J* = 7.6 Hz, 4H, Ph), 4.19 (s, 3H, CH₃) ppm.

¹³C NMR (176 MHz, CDCl₃, 25°C, TMS) δ 148.70 (Ht), 143.26 (Ht), 134.87 (Ht), 132.19 (Ht), 131.02, 130.78, 128.09, 127.76, 126.54, 120.83, 119.00, 49.31 (CH₃) ppm.

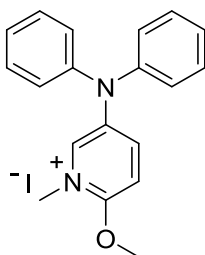


6-methoxy-N,N-diphenylpyridin-3-amine (4): diphenylamine (0.5g, 2.5mmol), 5-bromo-2-methoxypyridine (0.515g, 2.7mmol), palladium (II) acetate (0.028g, 0.13mmol), tri-tert-butylphosphonium tetrafluoroborate (0.1g, 0.39mmol) and sodium tertbutoxide (0.36g, 3.8mmol) were dissolved in anhydrous toluene (3ml) under argon atmosphere. The mixture was heated at 111°C for 4hours. Afterwards the reaction mixture was cooled to room temperature and filtered through a layer of celite. The crude product was purified by column chromatography (3/47 v/v acetone/*n*-hexane) to give **4** as green amorphous powder (0.51g, 66%).

Elemental Analysis calcd (%) for C₁₈H₁₆N₂O (276,34g/mol): C 78.24; H 5.84; N 10.14; O 5.79; found: C 78.36, H 5.71, N 10.25.

¹H NMR (400 MHz, Acetone-d₆, 25°C, TMS) δ 7.94 (d, *J* = 2.7 Hz, 1H, Ht), 7.48 (dd, *J* = 8.8, 2.8 Hz, 1H, Ht), 7.32 – 7.25 (m, 4H, Ar), 7.05 – 6.99 (m, 6H, Ph), 6.79 (d, *J* = 8.8 Hz, 1H, Ht), 3.89 (s, 3H, OCH₃) ppm.

^{13}C NMR (101 MHz, Acetone- d_6 , 25°C, TMS) δ 160.65 (Ht), 147.83 (Ht), 144.29 (Ht), 138.19 (Ht), 137.11 (Ht), 129.36, 122.68, 122.43, 111.26, 52.80 (OCH₃) ppm.

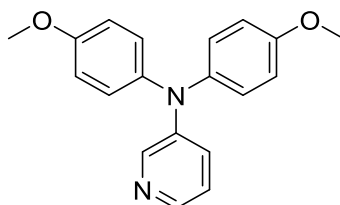


5-(diphenylamino)-2-methoxy-1-methylpyridin-1-ium iodide (5): a mixture of **4** (0.2g, 0.65mmol) and methyl iodide (0.647g, 4.5mmol) were dissolved in methanol (3ml). The reaction was conducted at room temperature for 72hours. Afterwards the reaction mixture was poured to 40ml of hexane and was cooled to -5°C for 1hour, forming precipitate which later on was filtrated giving amorphous yellow powder (0.04g, 14%).

Elemental analysis calcd (%) for C₁₉H₁₉IN₂O (418,28g/mol): C 54.56; H 4.58; I 30.34; N 6.70; O 3.82; found: C 54.42, H 4.48, N 6.81.

^1H NMR (400 MHz, Acetone- d_6 , 25°C, TMS) δ 7.55 (d, J = 2.8 Hz, 1H, Ht), 7.35–7.23 (m, 5H, Ar), 7.06–6.95 (m, 6H, Ar), 6.48 (d, J = 9.6 Hz, 1H, Ht), 3.48 (s, 3H, OCH₃), 2.93 (s, 3H, CH₃) ppm.

^{13}C NMR (101 MHz, Acetone- d_6 , 25°C, TMS) δ 147.57 (Ht), 141.21 (Ht), 138.02 (Ht), 129.28, 126.63, 122.68, 122.07, 121.77, 120.61, 53.18 (OCH₃), 36.55 (CH₃) ppm.

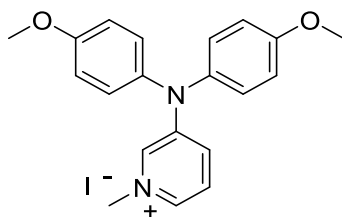


N,N-bis(4-methoxyphenyl)pyridin-3-amine (6): 3-bromopyridine (1g, 6.33mmol), 4,4-dimethoxydiphenylamine (1.74g, 7.6mmol), 2nd Generation XPhos precatalyst (0.049g, 0.0633mmol) and sodium tertbutoxide (0.912g, 9.5mmol) were dissolved in anhydrous dioxane (15ml) under argon atmosphere. The mixture was heated at 101°C for 14hours. Afterwards the reaction mixture was cooled to room temperature and filtered through a layer of celite. The crude product was purified by column chromatography (2/23 v/v acetone/*n*-hexane) to give **6** as brown oil (0.94 g, 49%).

Elemental analysis calcd (%) for C₁₉H₁₈N₂O₂ (306.37g/mol): C 74.49, H 5.92, N 9.14, O 10.44; found: C 74.38, H 6.01, N 9.38.

^1H NMR (700 MHz, MeOD, 25°C, TMS) δ 8.00 (d, J = 2.3 Hz, 1H, Ht), 7.93 (d, J = 4.2 Hz, 1H, Ht), 7.23 (ddd, J = 8.5, 2.7, 1.3 Hz, 1H, Ht), 7.17 (dd, J = 8.4, 4.6 Hz, 1H, Ht), 7.08 – 7.05 (m, 4H, Ph), 6.93 – 6.90 (m, 4H, Ph), 3.78 (s, 6H, OCH₃) ppm.

^{13}C NMR (176 MHz, MeOD, 25°C, TMS) δ 157.09, 146.02 (Ht), 139.66 (Ht), 139.30 (Ht), 139.14 (Ht), 126.80, 125.83, 123.80, 114.82, 54.56 (OCH₃) ppm.

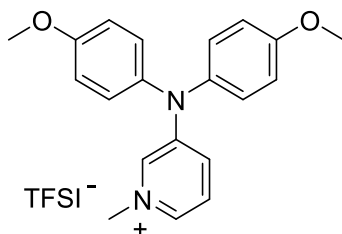


3-[bis(4-methoxyphenyl)amino]-1-methylpyridin-1-ium iodide (7): a mixture of *N,N*-bis(4-methoxyphenyl)pyridin-3-amine (0.5g, 1.6mmol) and methyl iodide (0.341g, 2.4mmol) were dissolved in anhydrous DMF (6ml). The reaction was conducted at room temperature for 14hours. Afterwards the reaction mixture was poured to 100ml of diethyl ether and was cooled to -5°C for 1hour, forming a layer of oil which later on was separated by decantation giving amorphous yellow oil as pure product **7** (0.33g, 46%).

Elemental analysis calcd (%) for C₂₀H₂₁IN₂O₂ (448.06g/mol): C 53.58, H 4.72, I 28.31, N 6.25, O 7.14; found: C 53.73, H 4.48, N 6.11.

^1H NMR (700 MHz, CDCl₃, 25°C, TMS) δ 8.57 (d, J = 5.6 Hz, 1H, Ht), 7.70 (s, 1H, Ht), 7.65 (dd, J = 9.0, 5.7 Hz, 1H, Ht), 7.54 (dd, J = 8.9, 2.3 Hz, 1H, Ar), 7.28-7.26 (m, 4H, Ph), 6.97 (d, J = 8.9 Hz, 4H, Ph), 4.42 (s, 3H, CH₃), 3.83 (s, 6H, OCH₃) ppm.

^{13}C NMR (176 MHz, CDCl₃, 25°C, TMS) δ 158.75, 148.94 (Ht), 135.77 (Ht), 134.33 (Ht), 130.82 (Ht), 128.90, 128.86, 128.10, 127.86, 116.07, 55.64 (OCH₃), 50.21 (CH₃) ppm.

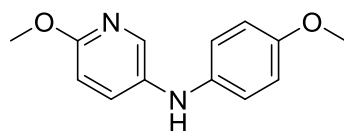


3-[bis(4-methoxyphenyl)amino]-1-methylpyridin-1-ium bis(trifluoromethanesulfonyl)azanide (8): 3-[bis(4-methoxyphenyl)amino]-1-methylpyridin-1-ium iodide (0.14g, 0.31mmol) and LiTFSI (0.18g, 0.62mmol) were dissolved in a mixture of DCM (2ml) and distilled H₂O (2ml). The reaction was conducted at room temperature for 24hours. Afterwards the solvent was removed leaving an amorphous mass, which then was washed with distilled H₂O giving the pure product **8** as a yellow oil (0.14g, 83%).

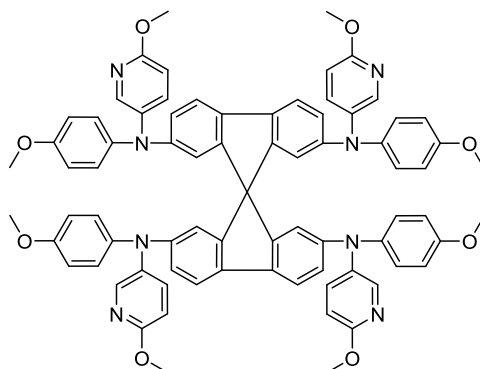
Elemental analysis calcd (%) for C₂₂H₂₁F₆N₃O₆S₂ (601.08g/mol): C 43.93, H 3.52, F 18.95, N 6.99, O 15.96, S 10.66; found: C 44.05, H 2.88, N 8.08.

$^1\text{H NMR}$ (700 MHz, CDCl_3 , 25°C, TMS) δ 7.93 (d, $J = 5.3$ Hz, 1H, Ht), 7.62 (s, 1H, Ht), 7.57 – 7.51 (m, 2H, Ht), 7.21 (t, $J = 6.1$ Hz, 4H, Ph), 6.97 (t, $J = 6.0$ Hz, 4H, Ph), 4.17 (s, 3H, CH_3), 3.82 (s, 6H, OCH_3) ppm.

$^{13}\text{C NMR}$ (176 MHz, CDCl_3 , 25°C, TMS) δ 159.03, 149.46 (Ht), 135.75 (Ht), 133.48 (Ht), 130.47 (Ht), 128.83, 128.13, 127.85, 116.23, 55.72 (OCH_3), 49.23 (CH_3) ppm.



6-methoxy-*N*-(4-methoxyphenyl)pyridin-3-amine (9): was synthesized according to an earlier reported procedure [32].

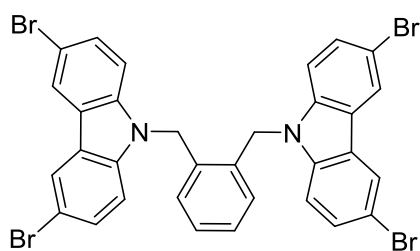


N^2,N^2',N^7,N^7' -tetrakis(4-methoxyphenyl)- N^2,N^2',N^7,N^7' -tetrakis(6-methoxypyridin-3-yl)-9,9'-spirobi[fluorene]-2,2',7,7'-tetramine (10): 2,2',7,7'-Tetrabromo-9,9'-spirobi[9H-fluorene] (0.5g, 0.79mmol), **9** (0.775g, 0.95mmol), palladium (II) acetate (0.009g, 0.04mmol), tri-tert-butylphosphonium tetrafluoroborate (0.0255g, 0.087mmol) and sodium tertbutoxide (0.455g, 4.7mmol) were dissolved in anhydrous toluene (6ml) under argon atmosphere. The mixture was heated at 111°C for 18hours. Afterwards the reaction mixture was cooled to room temperature and filtered through a layer of celite. The crude product was purified by column chromatography (5/20 v/v acetone/*n*-hexane) to give **10** as yellow amorphous powder (0.45g, 46%).

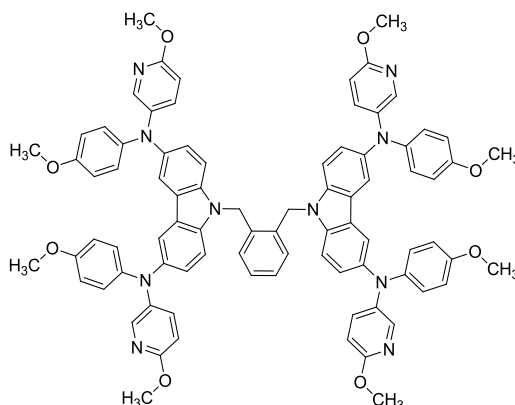
Elemental analysis calcd (%) for $\text{C}_{77}\text{H}_{64}\text{N}_8\text{O}_8$ (1229.41g/mol): C 75.23, H 5.25, N 9.11, O 10.41; found: C 75.09, H 5.37, N 9.28.

$^1\text{H NMR}$ (700 MHz, DMSO, 25°C, TMS) δ 7.73 (d, $J = 2.7$ Hz, 4H, Ht), 7.55 (d, $J = 8.3$ Hz, 4H, Ht), 7.32 (dd, $J = 8.8, 2.8$ Hz, 4H, Ht), 6.89 (dd, $J = 19.6, 9.1$ Hz, 19H, Ph), 6.77 (d, $J = 8.8$ Hz, 5H, Ph), 6.75 (d, $J = 1.9$ Hz, 2H, Ph), 6.74 (d, $J = 2.0$ Hz, 1H, Ph), 3.80 (s, 12H, OCH_3), 3.72 (s, 12H, OCH_3) ppm.

$^{13}\text{C NMR}$ (176 MHz, DMSO, 25°C, TMS) δ 159.93 (Ht), 156.10 (Ht), 149.93, 147.46, 142.61, 140.25, 138.72, 136.27, 134.86, 126.08, 121.58, 121.14, 116.27, 115.37, 111.51, 55.69 (OCH_3), 53.73 (OCH_3) ppm.



9,9'-[1,2-phenylenebis(methylene)]bis(3,6-dibromo-9H-carbazole) (11): was synthesized according to an earlier reported procedure [33].

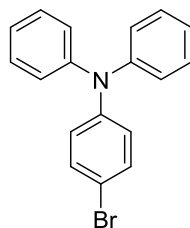


9,9'-[1,2-phenylenebis(methylene)]bis[*N*³,*N*⁶-bis(4-methoxyphenyl)-*N*³,*N*⁶-bis(6-methoxypyridin-3-yl)-9H-carbazole-3,6-diamine] (12): 9,9'-[1,2-phenylenebis(methylene)]bis(3,6-dibromo-9H-carbazole) (1.2g, 1.6mmol), 6-methoxy-*N*-(4-methoxyphenyl)pyridin-3-amine (1.542g, 6.7mmol), palladium (II) acetate (0.018g, 0.08mmol), tri-*tert*-butylphosphonium tetrafluoroborate (0.051g, 0.174mmol) and sodium *tert*butoxide (0.918g, 9.6mmol) were dissolved in anhydrous toluene (10ml) under argon atmosphere. The mixture was heated at 111°C for 9hours. Afterwards the reaction mixture was cooled to room temperature and filtered through a layer of celite. The crude product was purified by column chromatography (5/20 v/v acetone/*n*-hexane) to give **12** as yellow amorphous powder (0.90g, 42%).

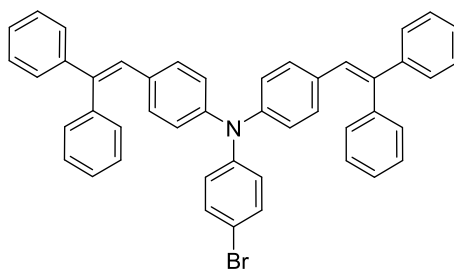
Elemental analysis calcd (%) for C₈₄H₇₂N₁₀O₈ (1349.5g/mol): C 74.76, H 5.38, N 10.38, O 9.48; found: C 74.62, H 5.50, N 10.51.

¹H NMR (700 MHz, DMSO-d₆, 25°C, TMS) δ 7.86 (d, *J* = 2.0 Hz, 4H, Ht), 7.76 (d, *J* = 2.8 Hz, 4H, Ar), 7.46 (d, *J* = 8.8 Hz, 4H, Ht), 7.33 (dd, *J* = 8.9, 2.9 Hz, 4H, Ht), 7.15 (dd, *J* = 8.7, 2.0 Hz, 4H, Ar), 7.03 (dd, *J* = 5.6, 3.3 Hz, 2H, Ph), 6.91–6.89 (m, 9H, Ar), 6.83–6.82 (m, 9H, Ar), 6.71 (d, *J* = 8.9 Hz, 4H, Ar), 5.84 (s, 4H, CH₂), 3.77 (s, 12H, OCH₃), 3.69 (s, 12H, OCH₃) ppm.

^{13}C NMR (176 MHz, DMSO- d_6 , 25°C, TMS) δ 159.04 (Ht), 155.06 (Ht), 141.91, 140.90, 140.35, 140.14, 138.22, 135.13, 134.68, 124.71, 124.20, 123.48, 117.54, 115.29, 111.28, 55.66 (OCH₃), 53.57 (OCH₃), 43.97 (CH₂) ppm.



4-bromo-*N,N*-diphenylaniline (13): was synthesized according to an earlier reported procedure [34].

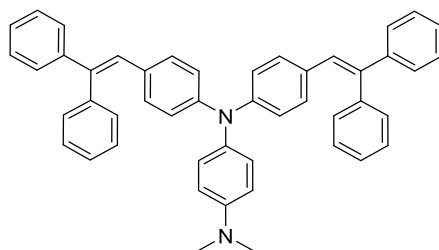


4-bromo-*N,N*-bis[4-(2,2-diphenylethenyl)phenyl]aniline (14): a mixture of **13** (5g, 15.4mmol), diphenylacetaldehyde (6.66g, 34mmol) and camphor-10-sulfonic acid (β) (3.58g, 15.4mmol) were dissolved in toluene (40ml). The mixture was heated for 18hours at reflux. Afterwards the mixture was cooled to room temperature and extracted with ethyl acetate. The organic layer was dried over anhydrous Na₂SO₄, filtered, the solvent was removed. The crude product was purified by column chromatography (*n*-hexane) to give **14** as a yellowish amorphous powder (4.47 g, 39%).

Elemental analysis calcd (%) for C₄₆H₃₄BrN (680.69g/mol): C 81.17, H 5.03, Br 11.74, N 2.06; found: C 81.33, H 5.14, N 1.89.

^1H NMR (700 MHz, CDCl₃, 25°C, TMS) δ 7.35–7.33 (m, 4H, Ph), 7.31–7.27 (m, 12H, Ph), 7.25–7.21 (m, 6H, Ph), 6.89–6.85 (m, 8H), 6.76 (d, J = 8.7 Hz, 4H, Ph) ppm.

^{13}C NMR (176 MHz, CDCl₃, 25°C, TMS) δ 146.27, 145.51, 143.38, 141.28, 140.54, 132.18, 130.45, 130.19, 128.77, 128.18, 127.41, 127.34, 127.30, 125.89, 123.24, 115.47 ppm.



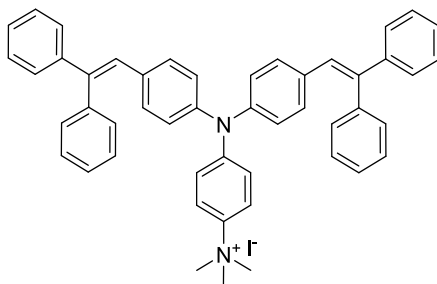
***N',N'*-bis[4-(2,2-diphenylethenyl)phenyl]-*N,N'*-dimethylbenzene-1,4-diamine (15)**: a mixture of **14** (0.3g, 0.44mmol), dimethyl amine hydrochloride (0.054g, 0.66mmol), 2nd

Generation XPhos precatalyst (0.007g, 0.0088mmol) and sodium tertbutoxide (0.123g, 1.32mmol) were dissolved in anhydrous dioxane (3.5ml) under argon atmosphere. The reaction was conducted in a microwave reactor for 3hours (130°C, power 200W, pressure 3 atm.). Afterwards the reaction mixture was cooled to room temperature and filtered through a layer of celite. The crude product was purified by column chromatography (1/49 v/v THF/*n*-hexane) to give **15** as a yellowish amorphous powder (0.12 g, 42%).

Elemental analysis calcd (%) for C₄₈H₄₀N₂ (644.87g/mol): C 89.40, H 6.25, N 4.34; found: C 89.65, H 6.13, N 4.22.

¹H NMR (700 MHz, DMSO, 25°C, TMS) δ 7.42 (dd, *J* = 10.3, 4.6 Hz, 4H, Ph), 7.38–7.35 (m, 2H, Ph), 7.34–7.30 (m, 4H, Ph), 7.28–7.24 (m, 6H, Ph), 7.16–7.15 (m, 4H, Ph), 6.99 (s, 2H, CH), 6.87–6.86 (m, 2H, Ph), 6.82 (d, *J* = 8.8 Hz, 4H, Ph), 6.69–6.68 (m, 2H, Ph), 6.61 (d, *J* = 8.8 Hz, 4H), 2.87 (s, 6H, N(CH₃)₂) ppm.

¹³C NMR (176 MHz, DMSO, 25°C, TMS) δ 148.61, 146.47, 143.06, 140.73, 139.93, 135.09, 130.62, 130.46, 130.10, 129.54, 128.78, 128.37, 127.97, 127.67, 127.59, 127.16, 121.18, 113.92, 40.67 (N(CH₃)₂) ppm.

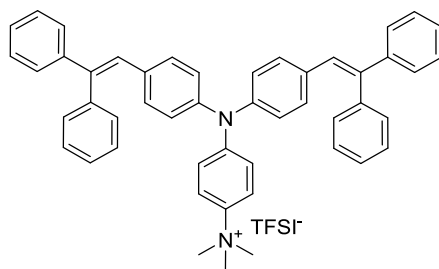


4-{bis[4-(2,2-diphenylethenyl)phenyl]amino}-*N,N,N*-trimethylanilinium iodide (16): *N*¹,*N*¹-bis[4-(2,2-diphenylethenyl)phenyl]-*N*⁴,*N*⁴-dimethylbenzene-1,4-diamine (0.32g, 0.5mmol) and methyl iodide (0.142g, 1mmol) were dissolved in anhydrous DMF (6ml). The reaction was conducted at room temperature for 24hours. Afterwards the reaction mixture was poured to 60ml of diethyl ether and was cooled to -5°C for 1hour, forming precipitate which later on was filtered, giving amorphous yellow crystals (0.38g, 98.3%, m. p. 143.0-145.5°C).

Elemental analysis calcd (%) for C₄₉H₄₃IN₂ (786.81g/mol): C 74.80, H 5.51, I 16.13, N 3.56; found: C 74.59, H 5.38, N 3.70.

¹H NMR (700 MHz, CDCl₃, 25°C, TMS) δ 7.65 (d, *J* = 9.4 Hz, 2H, Ph), 7.36 (t, *J* = 7.3 Hz, 4H, Ph), 7.33–7.29 (m, 10H, Ph), 7.28–7.26 (m, 2H, Ph), 7.23–7.22 (m, 4H, Ph), 7.06 (d, *J* = 9.4 Hz, 2H, Ph), 6.92–6.90 (m, 6H, Ph), 6.80 (d, *J* = 8.6 Hz, 4H, Ph), 3.95 (s, 9H, N(CH₃)₃) ppm.

¹³C NMR (176 MHz, CDCl₃, 25°C, TMS) δ 149.12, 144.34, 143.23, 142.21, 140.35, 139.70, 133.86, 130.79, 130.17, 128.84, 128.23, 127.54, 127.50, 127.43, 127.04, 124.63, 122.20, 120.51, 57.93 (N(CH₃)₃) ppm.



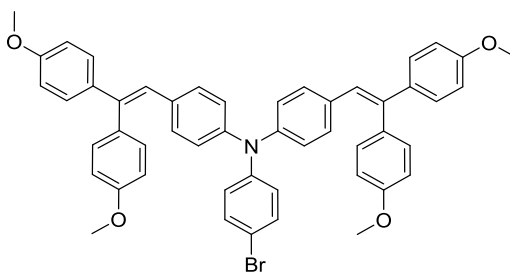
4-{bis[4-(2,2-diphenylethenyl)phenyl]amino}-*N,N,N*-trimethylanilinium

bis(trifluoromethanesulfonyl)azanide (17): 4-{bis[4-(2,2-diphenylethenyl)phenyl]amino}-*N,N,N*-trimethylanilinium iodide (0.28g, 0.36mmol) and LiTFSI (0.123g, 0.43mmol) were dissolved in a mixture of DCM (2ml) and methanol (2ml). The reaction was conducted at room temperature for 16hours. Afterwards the mixture was extracted with DCM and the solvent was removed giving the pure product **17** as yellow amorphous powder (0.314g, 94%).

Elemental analysis calcd (%) for $C_{51}H_{43}F_6N_3O_4S_2$ (940.06g/mol): C 65.16, H 4.61, F 12.13, N 4.47, O 6.81, S 6.82; found: C 64.94, H 4.49, N 4.66.

1H NMR (700 MHz, $CDCl_3$, 25°C, TMS) δ 7.38–7.29 (m, 18H, Ph), 7.22–7.21 (m, 4H, Ph), 7.05–7.03 (m, 2H, Ph), 6.94–6.91 (m, 6H, Ph), 6.81 (d, $J = 8.6$ Hz, 4H, Ph), 3.59 (s, 9H, $N(CH_3)_3$) ppm.

^{13}C NMR (176 MHz, $CDCl_3$, 25°C, TMS) δ 144.19, 143.19, 142.34, 140.33, 134.03, 130.81, 130.16, 128.82, 128.24, 127.55, 127.43, 127.00, 124.68 124.60, 122.10, 119.81, 57.71 ($N(CH_3)_3$) ppm.

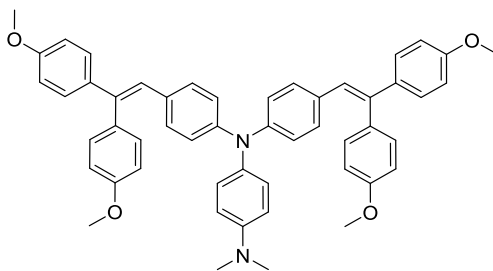


4-[2,2-bis(4-methoxyphenyl)ethenyl]-*N*-{4-[2,2-bis(4-methoxyphenyl)ethenyl]phenyl}-*N*-(4-bromophenyl)aniline (18): 4-bromo-*N,N*-diphenylaniline (5g, 15.4mmol), 2,2-bis(4-methoxyphenyl)acetaldehyde (8.69g, 33.9mmol) and camphor-10-sulfonic acid (β) (3.58g, 15.4mmol) were dissolved in toluene (50ml). The mixture was heated for 24hours at reflux. Afterwards the mixture was cooled to room temperature and extracted with ethyl acetate. The organic layer was dried over anhydrous Na_2SO_4 , filtered, the solvent was removed. The crude product was purified by column chromatography (2/23 v/v acetone/*n*-hexane) to give **18** as a yellowish green amorphous powder (4.94 g, 40%).

Elemental analysis calcd (%) for $C_{50}H_{42}BrNO_4$ (800.8g/mol): C 74.99, H 5.29, Br 9.98, N 1.75, O 7.99; found: C 75.28, H 5.16, N 1.62.

1H NMR (700 MHz, DMSO- d_6 , 25°C, TMS) δ 7.52–7.36 (m, 2H, Ph), 7.28–7.12 (m, 4H, Ph), 7.10–6.78 (m, 21H, Ph), 6.76–6.69 (m, 2H, Ph), 6.68 (d, J = 8.6 Hz, 1H, Ph), 3.79–3.70 (m, 12H, OCH₃) ppm.

^{13}C NMR (176 MHz, DMSO- d_6 , 25°C, TMS) δ 159.26, 159.03, 145.08, 140.41, 135.91, 131.30, 130.91, 130.66, 128.64, 125.99, 125.90, 125.86, 125.76, 123.56, 114.84, 114.16, 55.60 (OCH₃), 55.47 (OCH₃) ppm.

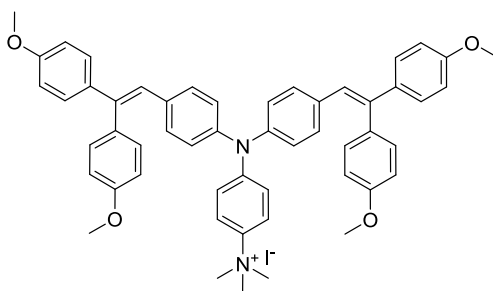


***N*¹,*N*¹-bis{4-[2,2-bis(4-methoxyphenyl)ethenyl]phenyl}-*N*⁴,*N*⁴-dimethylbenzene-1,4-diamine (19):** compound **18** (0.3g, 0.38mmol), dimethyl amine hydrochloride (0.046g, 0.56mmol), 2nd Generation XPhos precatalyst (0.006g, 0.0075mmol) and sodium tertbutoxide (0.108g, 1.32mmol) were dissolved in anhydrous dioxane (3ml) under argon atmosphere. The reaction was conducted in a microwave reactor for 3hours (130°C, power 200W, pressure 3 atm.). Afterwards the reaction mixture was cooled to room temperature and filtered through a layer of celite. The crude product was purified by column chromatography (1/4 v/v THF/*n*-hexane) to give **19** as yellowish powder (0.115 g, 40%).

Elemental analysis calcd (%) for $C_{52}H_{48}N_2O_4$ (764.97g/mol): C 81.65, H 6.32, N 3.66, O 8.37; found: C 81.39, H 6.24, N 3.75.

1H NMR (700 MHz, DMSO- d_6 , 25°C, TMS) δ 7.19–7.17 (m, 2H, Ph), 7.06–7.04 (m, 5H, Ph), 6.98–6.95 (m, 5H, Ph), 6.90–6.82 (m, 12H, Ph), 6.76–6.68 (m, 4H, Ph), 6.62 (d, J = 8.7 Hz, 2H, Ph), 3.78–3.75 (m, 12H, OCH₃), 2.89–2.87 (m, 6H, N(CH₃)₂) ppm.

^{13}C NMR (176 MHz, DMSO- d_6 , 25°C, TMS) δ 159.12, 158.96, 146.13, 139.37, 136.05, 132.84, 131.46, 131.33, 130.97, 130.81, 130.33, 128.50, 128.29, 125.59, 121.23, 114.86, 114.16, 55.61 (OCH₃), 55.49 (OCH₃), 49.07 (N(CH₃)₃) ppm.

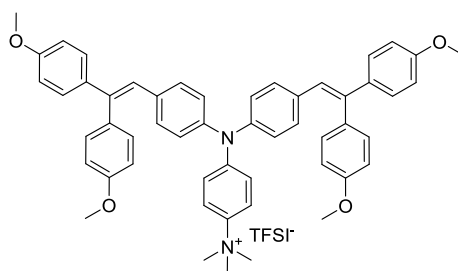


4-(bis{4-[2,2-bis(4-methoxyphenyl)ethenyl]phenyl}amino)-*N,N,N*-trimethylanilinium iodide (20): a mixture of **19** (0.36g, 0.47mmol) and methyl iodide (0.233g, 1.65mmol) were dissolved in anhydrous DMF (6.5ml). The reaction was conducted at room temperature for 18hours. Afterwards the reaction mixture was poured to 65ml of diethyl ether and was cooled to -5°C for 1hour, forming precipitate which was filtered giving amorphous yellow powder (0.424g, 99.3%).

Elemental analysis calcd (%) for C₅₃H₅₁IN₂O₄ (906.91g/mol): C 70.19, H 5.67, I 13.99, N 3.09, O 7.06; found: C 70.01, H 5.42, N 3.24.

¹H NMR (700 MHz, CDCl₃, 25°C, TMS) δ 7.29–7.21 (m, 5H, Ph), 7.17–7.09 (m, 6H, Ph), 7.06 (d, *J* = 9.3 Hz, 1H, Ph), 6.98–6.92 (m, 5H, Ph), 6.90 – 6.76 (m, 13H, Ph), 3.99–3.91 (m, 9H, N(CH₃)₃), 3.85–3.80 (m, 12H, OCH₃) ppm.

¹³C NMR (176 MHz, CDCl₃, 25°C, TMS) δ 162.54, 159.26, 159.00, 149.27, 143.94, 141.48, 139.43, 136.26, 134.41, 132.70, 131.57, 131.41, 130.75, 130.66, 130.58, 128.71, 125.15, 124.72, 121.94, 120.38, 114.19, 113.59, 57.92 (N(CH₃)₃), 55.34 (OCH₃), 55.29 (OCH₃), 55.24 (OCH₃), 55.18 (OCH₃) ppm.



4-(bis{4-[2,2-bis(4-methoxyphenyl)ethenyl]phenyl}amino)-*N,N,N*-trimethylanilinium bis(trifluoromethanesulfonyl)azanide (21): 4-(bis{4-[2,2-bis(4-methoxyphenyl)ethenyl]phenyl}amino)-*N,N,N*-trimethylanilinium iodide (0.2g, 0.22mmol) and LiTFSI (0.076g, 0.264mmol) were dissolved in a mixture of DCM (3ml) and methanol (3ml). The reaction was conducted at room temperature for 24hours. Afterwards the mixture was extracted with DCM and the solvent was removed giving the pure product **21** as dark green amorphous powder (0.21g, 90%).

Elemental analysis calcd (%) for $C_{56}H_{51}F_6N_3O_8S_2$ (1060.16g/mol): C 62.50, H 5.15, F 10.59, N 3.90, O 11.89, S 5.96; found: C 62.38, H 5.02, N 4.00.

1H NMR (700 MHz, $CDCl_3$, 25°C, TMS) δ 7.37–7.34 (m, 2H, Ph), 7.14–7.11 (m, 5H, Ph), 7.02–7.01 (m, 3H, Ph), 7.00–6.94 (m, 6H, Ph), 6.90–6.87 (m, 6H, Ph), 6.86 – 6.80 (m, 6H, Ph), 6.70 – 6.66 (m, 2H, Ph), 3.83 – 3.80 (m, 12H, OCH_3), 3.64–3.60 (m, 9H, $N(CH_3)_3$) ppm.

^{13}C NMR (176 MHz, $CDCl_3$, 25°C, TMS) δ 159.30, 159.03, 149.64, 149.54, 143.75, 141.65, 136.21, 134.64, 132.67, 131.55, 131.40, 130.76, 130.66, 130.62, 128.72, 125.08, 124.80, 121.79, 119.70, 114.17, 113.61, 57.77 ($N(CH_3)_3$), 55.34 (OCH_3), 55.24 (OCH_3), 55.18 (OCH_3) ppm.

5. Results and conclusions

- New quaternary ammonium salts have been synthesized, their thermal, photoelectric and optical properties have been investigated.
- Ionic HTMs were obtained in high yields.
- Pyridine moieties tend to lower T_g and T_m of the investigated compounds.
- The introduction of iodine anion leads either to a formation of a crystalline structure or the increase of T_m , while the addition of TFSI has the opposite effect.
- Addition of methoxy groups has no effect on the absorption spectra maximum in case of HTMs **19-21**.
- Addition of ionic groups leads to a hypsochromic shift and hyperchromic effect.
- Introduction of donoric methoxy groups lowers I_p for compounds **19-21**.
- The formation of quaternary ammonium groups increases the I_p of compounds, possibly due to the decrease of the amino group donor properties.
- Poor performances of doped HTMs in PSC devices **10, 12, 15** and **19** could be attributed to their spatial structure and fairly high I_p .
- Low conductivity and high I_p makes ionic HTMs unsuitable for PSC applications.
- HTMs **15** and **19** give hope that with the proper device optimization they could be used efficiently in PSC.

List of publications

1. Matsui, T., Petrikyte, I., Malinauskas, T., Domanski, K., Daskeviciene, **M.**, **Steponaitis**, M., Gratia, P., Tress, W., Correa-Baena, J. P., Abate, A., Hagfeldt, A., Grätzel, M., Nazeeruddin, M. K., Getautis, V. and Saliba, M. Additive-Free Transparent Triarylamine-Based Polymeric Hole-Transport Materials for Stable Perovskite Solar Cells. *Chemsuschem*, 2016, vol. 9, p 2567–2571.

Acknowledgments

My sincere thanks to **Asoc. Prof. Dr. T. Malinauskas** for passing onto me a great amount of knowledge and skills as well as for the creation of friendly working environment.

A great amount of gratitude is expressed to **Prof. Dr. V. Getautis** (Department of Organic Chemistry, Kaunas University of Technology) for the opportunity to work in his research group.

I would like to thank **Dr. S. Urnikaitė** for practical advice throughout my studies.

I am grateful to **I. Liutvinienė, L. Pečiulytė, A. Beliauskas, G. Ragaitė** for UV-vis, DSC, NMR measurements.

Gratitude is expressed to **Prof. Habil. Dr. V. Gaidelis** and **Dr. V. Jankauskas** from the Department of Solid State Electronics, Vilnius University for the measurements of ionization potentials and charge carrier mobilities.

I thank **Dr. Michael Saliba** from EPFL University, Lausanne, Switzerland for the fabrication and characterization of the solar cells.

I am grateful to **Prof. H. Snaith** and **Dr. N. Sakai** from University of Oxford Department of Physics, Oxford, England for passing onto me the knowledge of the fabrication of perovskite solar cells.

References

1. Powell, D. M., Winkler, M. T., Choi, H. J., Simmons, C. B., Needleman, D. B., Buonassisi, T. Crystalline silicon photovoltaics: a cost analysis framework for determining technology pathways to reach baseload electricity costs. *Energy Environ. Sci.*, 2012, vol. 5, p. 5874.
2. Manser, J. S., Christians, J. A., Kamat, P. V. Intriguing Optoelectronic Properties of Metal Halide Perovskites. *Chemical Reviews*, 2016 vol. 116, p. 12956–13008.
3. Mitzi, D. B., Feild, C. A., W. T. A. Harrison, W. T. A., Guloy, A. M., Conducting tin halides with a layered organic-based perovskite structure. *Nature*, 1994, 369, p. 467–469.
4. Mitzi, D. B.; Wang, S.; Feild, C. A.; Chess, C. A.; Guloy, A. M.; Conducting Layered Organic-inorganic Halides Containing <110>-Oriented Perovskite Sheets. *Science*, 1995, 267, 1473–1476.
5. Saliba, M., Matsui, T., Seo, J., Domanski, K., Correa-Baena, J. P., Nazeeruddin, M. K., Zakeeruddin, S.W., Tress, W., Abate, A., Hagfeldt, A., Grätzel, M. Cesium-containing triple cation perovskite solar cells: improved stability, reproducibility and high efficiency. *Energy Environ. Sci.*, 2016, vol. 9, p. 1989-1997.
6. NREL efficiency chart, [http://www.nrel.gov/ncpv/images/efficiency chart.jpg](http://www.nrel.gov/ncpv/images/efficiency%20chart.jpg), accessed: 05/08/2016.
7. Ooyama, Y., Y. Yarima. Molecular designs and syntheses of organic dyes for dye-sensitized solar cells. *European Journal of Organic Chemistry*, 18, 2009, p. 2903–2934.
8. Miyamoto, E., Yamaguchi, Y., Masaaki, M. *Electrophotography*, 1989, vol. 28, p. 364
9. . H.O. Wirth // *Angew. Makromol. Chem*, 1991, p. 185-186
10. Coropceanu, V., Cornil, J., da Silva Filho, D. A., Olivier, Y., Silbey, R., Brédas, J. L. Charge transport in organic semiconductors. *Chemical Reviews*, 2007, vol 107 (4), p. 926-952.
11. Bach, U.; Lupo, D.; Comte, P.; Moser, J. E.; Weissortel, F.; Salbeck, J.; Spreitzer, H.; Grätzel, M. Solid-state dye-sensitized mesoporous TiO₂ solar cells with high photon-to-electron conversion efficiencies. *Nature*, 1998, vol 395, p 583–585.
12. Snaith, H. J.; Grätzel, M. Enhanced charge mobility in a molecular hole transporter via addition of redox inactive ionic dopant: Implication to dye-sensitized solar cells. *Appl. Phys. Lett.*, 2006, vol 89, p 262114.

13. Abate, A.; Leijtens, T., Pathak, S., Teuscher, J., Avolio, R., Errico, M. E., Kirkpatrick, J., Ball, J. M., Docampo, P., McPherson, I., Snaith, H. J. Lithium salts as "redox active" p-type dopants for organic semiconductors and their impact in solid-state dye-sensitized solar cells. *Chem. Chem. Phys.*, 2013, vol 15, p. 2572.
14. Jeon, N. J., Noh, J. H., Yang, W. S., Kim, Y. C., Ryu, S., Seo, J., Seok, S. I. Compositional engineering of perovskite materials for high-performance Nature, 2015, 14133.
15. Zhao, X., Zhang, F., Yi, C., Bi, D., Bi, X., Wei, P., Luo, J., Liu, X., Wang, S., Li, X., S. M. and Grätzel, M. Novel one-step synthesized and dopant-free hole transport material for efficient and stable perovskite solar cells. *J. Mater. Chem. A*, 2016, vol. 4, p. 16330–16334.
16. Qi, P., Zhang, F., Zhao, X., Liu, X., Bi, X., Wei, P., Xiao, Y., Li, X. and Wang, S. Efficient, Stable, Dopant-Free Hole-Transport Material with a Triphenylamine Core for $\text{CH}_3\text{NH}_3\text{PbI}_3$ Perovskite Solar Cells. *Energy Technol.* 2017, vol. 5, p 1-6.
17. Ni, J. S., Hsieh, H. C., Chen, C. A., Wen, Y. S., Wu, W. T., Shih, Y.C., Lin, K. F., Wang, L., and Lin, J. T. Near-Infrared-Absorbing and Dopant-Free Heterocyclic Quinoid-Based Hole-Transporting Materials for Efficient Perovskite Solar Cells. *ChemSusChem* 2016, vol. 9, p. 3139-3144
18. Zhang, F., Liu, X., Yi, C., Bi, D., Luo, J., Wang, S., Li, X., Xiao, Y., Zakeeruddin, M. S. and Gratzel, M. Dopant-Free Donor (D)–p–D–p–D Conjugated Hole-Transport Materials for Efficient and Stable PerovskiteSolar Cells. *ChemSusChem* 2016, vol. 9, p. 2578-2585.
19. Zhang, J., Xu, B., Yang, L., Mingorance, A., Ruan, C., Hua, Y., Wang, L., Vlachopoulos, N., Cantú, M. L., Boschloo, G., Hagfeldt, A., Sun, L. and Johansson, E. M. J. Incorporation of Counter Ions in Organic Molecules: New Strategy in Developing Dopant-Free Hole Transport Materials for Efficient Mixed-Ion Perovskite Solar Cells. *Adv. Energy Mater.* 2017.
20. Kwon, Y. S., Lim, J., Yun, H. J., Kim, Y. H., and Park. T. Diketopyrrolopyrrole-Containing Hole Transporting Conjugated Polymer for use in Efficient Stable Organic-Inorganic Hybrid Solar Cells based on a Perovskite. *Energy Environ. Sci.*, 2013, vol 7, p 1454-1460.
21. Zhu, Z., Bai, Y., Lee, H. K. H., Mu, C., Zhang, T., Zhang, L., Wang, J., Yan, H., So, S. K. and Yang, S. Polyfluorene Derivatives are High-Performance Organic Hole-

- Transporting Materials for Inorganic–Organic Hybrid Perovskite Solar Cells. *Adv. Funct. Mater.*, 2014, vol. 24, p. 7357–7365.
22. Chen, W., Bao, X., Zhu, Q., Zhu, D., Qiu, M., Sun, M. and Yang, R. Simple Planar Perovskite Solar Cells with a Dopant-free Benzodithiophene Conjugated Polymer as Hole Transporting Material. *J. Mater. Chem. C*, 2015, vol. 3, p. 10070—10073.
 23. Kim, G. W., Kang, G., Kim, J., Lee, G. Y., Kim, H. I., Pyeon, L., Lee, J. and Park., T. Dopant-free polymeric hole transport materials for highly efficient and stable perovskite solar cells. *Energy Environ. Sci.*, 2016, vol. 9, p. 2326-2333.
 24. Matsui, T., Petrikyte, I., Malinauskas, T., Domanski, K., Daskeviciene, M., Steponaitis, M., Gratia, P., Tress, W., Correa-Baena, J. P., Abate, A., Hagfeldt, A., Grätzel, M., Nazeeruddin, M. K., Getautis, V. and Saliba, M. Additive-Free Transparent Triarylamine-Based Polymeric Hole-Transport Materials for Stable Perovskite Solar Cells. *Chemsuschem*, 2016, vol. 9, p 2567–2571.
 25. Li, C., Liu, M., Pschirer, N. G., Baumgarten, M., Mullen, K. Polyphenylene-Based Materials for Organic Photovoltaics. *Chem. Rev.* 2010, vol. 110, p. 6817.
 26. Yang, W. S., Noh, J. H., Jeon, N. J., Kim, Y. C., Ryu, S., Seo, J. and Seok, S. I. High-performance photovoltaic perovskite layers fabricated through intramolecular exchange. *Science*, 2015, vol. 348, p. 1234–1237.
 27. McMeekin, D. P., Sadoughi, G., Rehman, W., Eperon, G. E., Saliba, M., Horantner, M. T., Haghighirad, A., Sakai, N., Korte, L., Rech, B., Johnston, M. B., Herz, L. M. and Snaith, H. J. A mixed-cation lead mixed-halide perovskite absorber for tandem solar cells. *Science*, 2016, vol. 351, p. 151–155.
 28. Heckmann, A. and Lambert, C. Organic Mixed-Valence Compounds: A Playground for Electrons and Holes. *Angew. Chem. Int. Ed.*, 2012, vol. 51, p. 326 – 392.
 29. Izuhara, D. and Swager, T. M. Poly(Pyridinium Phenylene)s: Water-Soluble N-Type Polymers. *J. AM. CHEM. SOC.* 2009, vol. 131, p. 17724–17725.
 30. Cheng, M., Aitola, K., Chen, C., Zhang, F., Liu, P., Sveinbjörnsson, K., Hua, Y., Kloo, L., Boschloo, G., Sun, L. Acceptor–Donor–Acceptor Type Ionic Molecule Materials for Efficient Perovskite Solar Cells and Organic Solar Cells. *Nano Energy*. 2016, vol. 30, p. 387-397.
 31. Topchiy, M. A., Dzhevakov, P. B., Rubina, M.S., Morozov, O. S., Asachenko, A. F. and Nechaev, M. S. Solvent-Free Buchwald–Hartwig (Hetero)arylation of Anilines,

- Diarylamines, and Dialkylamines Mediated by Expanded-Ring N-Heterocyclic Carbene Palladium Complexes. *Eur. J. Org. Chem.* 2016, vol. 10, p. 1908–1914.
32. Hanthorn, J. J., Valgimigli, L. and Pratt, D. A. Preparation of Highly Reactive Pyridine - and Pyrimidine-Containing Diarylamine Antioxidants. *J. Org. Chem.*, 2012, vol. 77 (16), p 6908–6916.
33. Gratia, P., Magomedov, A., Malinauskas, T., Daskeviciene, M., Abate, A., Ahmad, S., Grätzel, M., Getautis, V. and Nazeeruddin, M. K. A Methoxydiphenylamine-Substituted Carbazole Twin Derivative: An Efficient Hole-Transporting Material for Perovskite Solar Cells. *Angew. Chem. Int. Ed.* 2015, 54, 11409 –11413.
34. Gudeika, D., Sini, G., Jankauskas, V., Sych, G. and Grazulevicius, J. V. Synthesis and properties of the derivatives of triphenylamine and 1,8-naphthalimide with the olefinic linkages between chromophores. *RSC Advances.* 2016, vol. 6(3), p. 2191-2201.